Appendix A.30:

Shortland St – CPT 6551

Table 1: Site Description for Shortland St (CC LIQ 13 – CPT 6551).

Attribute	Yes/No			Description/Date	Symbol in Figure 1
	10-m Buffer	20-m Buffer	50-m Buffer		
Near a body of surface water or other free face features?	No	No	No	The center of the site is ~490 m to the west from the Avon River. The height of the free face is ~1-1.5 m.	NA
Lateral spreading observed during the CES?	No	No	No	No ground cracks were observed by the mapping team.[1]	NA
Nearby buildings or structures?	No	Yes	Yes	Buildings occupy 3% and 18% of the 20-m and 50-m buffers, respectively. They are in all quadrants of the 50-m buffer and the SW quadrant of the 20-m buffer.	White Fill + Brown Outline
Sloping land?	No	Yes	Yes	The site is in the residential, generally level area. However, the access driveways at the properties are sloped due to the higher elevation of the properties relative to the road.	NA
Step changes in the ground surface?	No	Yes	Yes	Step changes are typically present between the front lawns on both sides of the street and the two sidewalks. The typical elevation difference is 0.5-1 m.	NA
Retaining walls?	No	Yes	Yes	Retained front lawns (typ. 0.5- to 1-m high).	NA
Vegetation?	No	Yes	Yes	Trees and bushes cover 13% and 14% of the 20-m and 50-m buffers, respectively. They are in all quadrants of the buffers.	White Fill + Green Outline
Anthropogenic changes to the site between the LiDAR surveys?	Yes	Yes	Yes	Building addition in the SE quadrant of the 50-m buffer between Sep 5, 2010 and Feb 7, 2011. Road construction in the NW, NE, and SE quadrants of all buffers between Jan 2013 and Mar 2013. Building removal in the SW quadrant of the 50-m buffer (50 Shortland St) between Sep 2013 and Feb 2014. Building addition at the same property between Feb 2014 and Aug 2014. Vegetation removal, fence addition, and possibly earthwork in the SW quadrant of the 20- and 50-m buffers (54 Shortland St) between Aug 2014 and Jan 2015. Building removal in the SE quadrant of the 50-m buffer between Jun 2015 and Jul 2015. Construction in the E portion of the 50-m buffer between Jul 2015 and Sep 2015.	Building Addition/Removal: Orange Outline; Vegetation Removal: Green Crossline
Other important factors?	Yes	Yes	Yes	Low-motor-vehicle-volume, two-way roadway (Shortland St) covers 53, 31, and 13% of the 10-, 20-, and 50-m buffers, respectively. It occupies the NW, NE, and SE quadrants of all buffers.	Road: Gray Fill + Red Outline

Notes: Buffer is the area within a circle of a specified radius with CPT investigations done at its center (172.693665°, -43.515402°).

[1] Canterbury Geotechnical Database. (2012). "Observed Ground Crack Locations", Map Layer CGD0400 - 23 July 2012, retrieved July 09, 2018 from https://canterburygeotechnicaldatabase.projectorbit.com/

Figure 1: Site plan with areas where ejecta-induced settlement is considered.

Note 1: Patch A (outlined in red) in free field was selected for settlement assessment as an area free of vegetation and structures. Other factors considered in the patch selection were its proximity to a CPT, a property subjected to addition and/or demolition of a structure, front yard/backyard alterations (e.g., ploughing, rubble, scrap), and aerial distribution of sediment ejecta. In addition, the entire portion of the road within the 50-m buffer was considered for settlement assessment. Roads as hard, relatively flat surfaces provide many ground-classified points. The LiDAR-based settlement analyses of Patch A were not conducted for any EQ event due to the evident absence of ejecta. Likewise, the LiDAR-based settlement analyses of the Road were not performed for the Sep-10 and Dec-11 EQs due to the evident absence of ejecta.

Table 2: LiDAR flight error adjustments, global adjustments for the difference between average LiDAR point elevations and benchmark survey elevations, and vertical tectonic movement adjustments.

	Adjustments (mm)		
Earthquake Event(s)	LiDAR Flight Error	Global Offset[2]	Tectonic Vertical Movement
Sep-10	0	-3	0
Feb-11	0	16	0
Jun-11	0	38	-50
Dec-11	-50	-65	0
CES	-50	-14	-50
Any LiDAR survey affected by ejecta?			No

Note: The negative sign indicates the subtraction from the ground surface subsidence, while the positive sign indicates the addition to the ground surface subsidence.

Table 3: LiDAR Measurement Error for Road.

Surveys	Buffer	Area Averaged Difference Indicating Repeat Measurement Error (mm)	σ*individual LiDAR points (mm)	%Reduction in σ due to Area Averaging of LiDAR Points
Post Feb 2011: Mar 2011 and May 2011	10-m	35	59	[59,95]
	20-m	37		
	50-m	56		
Post Dec 2011: Feb 2012 and Oct 2015	10-m	ND	70	[ND,ND]
	20-m	ND		
	50-m	ND		

*Standard deviation; ND = Not determined.

[2] Russell, J., & van Ballegooy, S. (2015). *Canterbury Earthquake Sequence: Increased liquefaction vulnerability assessment methodology*. New Zealand: Tonkin & Taylor Ltd.

Table 4: Ground surface subsidence adjustments due to LiDAR measurement error for Road.

Earthquake Event(s)	$\sigma_{pre\text{-}EQ\ LiDAR\ survey}$ (mm)	$\sigma_{post\text{-}EQ\ LiDAR\ survey}$ (mm)	σ_{total} (mm)	Area Average Adjusted σ (mm) **
Sep-10	158	56	134	±127
Feb-11	56	59	59	±56
Jun-11	59	61	62	±59
Dec-11	61	70	87	±82
CES	158	70	124	±118

**Based on the highest %Reduction in Table 3.

Table 5: Raw liquefaction-related ground surface subsidence using original LiDAR points for Road.

	Average Ground Surface Subsidence (mm)		
Earthquake Event(s)	10-m Buffer	20-m Buffer	50-m Buffer
Sep-10	ND	ND	ND
Feb-11	135	114	98
Jun-11	79	86	94
Dec-11	ND	ND	ND
CES	ND	ND	ND

Table 6: Corrected liquefaction-related ground surface subsidence using original LiDAR points for Road with the calculated adjustments in Table 2.

	Average Calculated Ground Surface Subsidence (mm)		
Earthquake Event(s)	10-m Buffer	20-m Buffer	50-m Buffer
Sep-10	ND	ND	ND
Feb-11	151±50	130±50	114±50
Jun-11	67±50	74±50	82±50
Dec-11	ND	ND	ND
CES	ND	ND	ND

Notes: Plus/minus values are same as those in Table 4, but rounded to the nearest 25; Positive overall values indicate ground surface subsidence, while negative overall values indicate ground surface uplift; ND = Not determined.

Table 7: Corrected liquefaction-related ground surface subsidence for Road using LiDAR DEMs.

	Estimated Ground Surface Subsidence (mm)								
	10-m Buffer			20-m Buffer			50-m Buffer		
Earthquake Event(s)	16th %ile	50th %ile	84th %ile	16th %ile	50th %ile	84th %ile	16th %ile	50th %ile	84th %ile
Sep-10	<50	<50	50	<50	<50	50	<50	<50	50
Feb-11	100	150	150	100	150	150	100	100	150
Jun-11	<50	<50	<50	<50	<50	<50	<50	<50	<50
Dec-11	<50	<50	50	<50	<50	50	<50	<50	50
CES	100	200	200	100	200	200	100	200	300

Note: These percentiles are not the exact statistical measures; they indicate the spatial variability of ground surface subsidence.

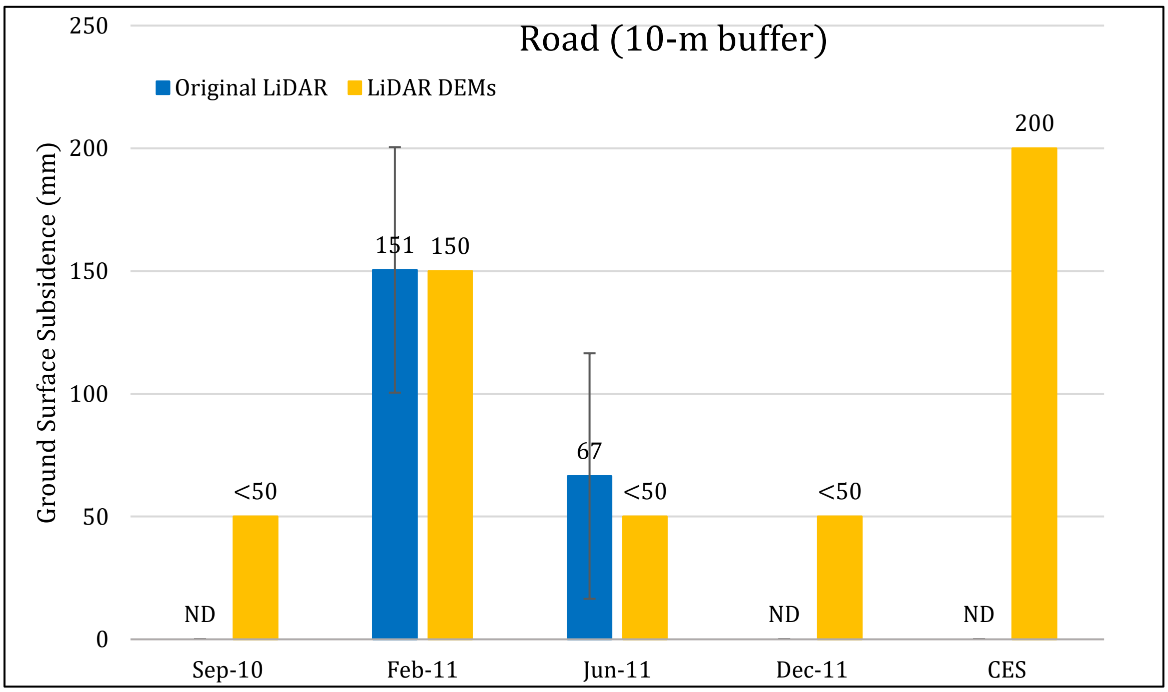

Figure 2: Comparison between ground surface subsidence determined from original LiDAR survey points and ground surface subsidence (50th %ile) estimated using LiDAR DEMs for Road (10-m buffer).

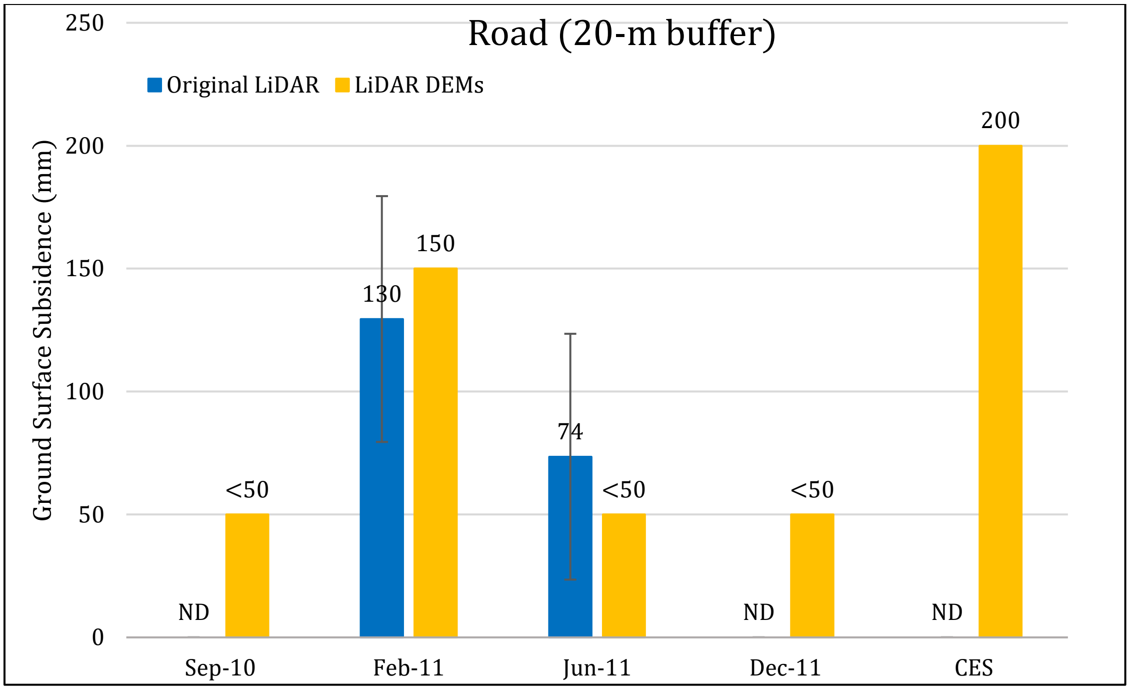

Figure 3: Comparison between ground surface subsidence determined from original LiDAR survey points and ground surface subsidence (50th %ile) estimated using LiDAR DEMs for Road (20-m buffer).

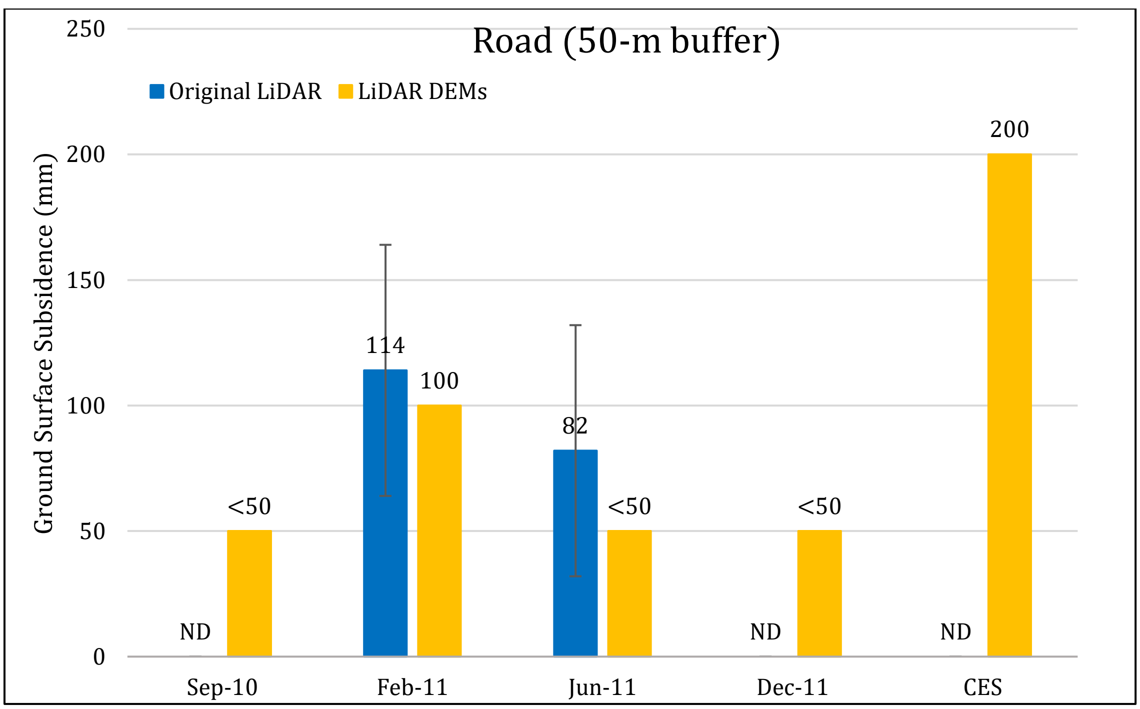

Figure 4: Comparison between ground surface subsidence determined from original LiDAR survey points and ground surface subsidence (50th %ile) estimated using LiDAR DEMs for Road (50-m buffer).

Note 2: The ground surface subsidence values determined from original LiDAR survey points are similar to the ground surface subsidence values estimated using LiDAR DEMs for all earthquake events.

Table 8a: Ejecta-Induced settlement for the top 20 m of the soil profile for Patch A (20- and 50-m buffers) for the 50th %ile PGA, P_L=50%, and C_{FC}=0.13 using BI-2014, ZRB-2002, and I_C cutoff of 2.6.

Earthquake Event(s)	M_W	PGA (g)	Depth to Groundwater (m)	S_T (mm)	S_{V1D} (mm)	$S_{E,L}$ (mm)
Sep-10	7.1	0.19	3.0	ND	13±20	ND
Feb-11	6.2	0.47	3.0	ND	107±50	ND
Jun-11	6.2	0.29	3.0	ND	45±25	ND
Dec-11	6.1	0.31	2.0	ND	70±50	ND

Notes: S_T = Total settlement (Table 6); S_{V1D} = Average vertical settlement due to volumetric compression using Boulanger and Idriss (2014) (BI-2014), Zhang et al. (2002) (ZRB-2002) procedures and de Greef and Lengkeek (2018) thin-layer correction; $S_{E,L}$ = Ejecta-induced settlement as the difference between the LiDAR-based S_T and S_{V1D}.

Table 8b: Ejecta-Induced settlement for the top 20 m of the soil profile for Road (20-m buffer) for the 50th %ile PGA, P_L=50%, and C_{FC}=0.13 using BI-2014, ZRB-2002, and I_C cutoff of 2.6.

Earthquake Event(s)	M_W	PGA (g)	Depth to Groundwater (m)	S_T (mm)	S_{V1D} (mm)	$S_{E,L}$ (mm)
Sep-10	7.1	0.19	3.0	ND	13±20	ND
Feb-11	6.2	0.47	3.0	130±50	107±50	23±71
Jun-11	6.2	0.29	3.0	74±50	45±25	29±56
Dec-11	6.1	0.31	2.0	ND	70±50	ND

Notes: S_T = Total settlement (Table 6); S_{V1D} = Average vertical settlement due to volumetric compression using Boulanger and Idriss (2014) (BI-2014), Zhang et al. (2002) (ZRB-2002) procedures and de Greef and Lengkeek (2018) thin-layer correction; $S_{E,L}$ = Ejecta-induced settlement as the difference between the LiDAR-based S_T and S_{V1D}.

Table 8c: Ejecta-Induced settlement for the top 20 m of the soil profile for Road (50-m buffer) for the 50th %ile PGA, P_L=50%, and C_{FC}=0.13 using BI-2014, ZRB-2002, and I_C cutoff of 2.6.

Earthquake Event(s)	M_W	PGA (g)	Depth to Groundwater (m)	S_T (mm)	S_{V1D} (mm)	$S_{E,L}$ (mm)
Sep-10	7.1	0.19	3.0	ND	14±20	ND
Feb-11	6.2	0.47	3.0	114±50	119±50	-5±71
Jun-11	6.2	0.29	3.0	82±50	50±25	32±56
Dec-11	6.1	0.31	2.0	ND	78±50	ND

Notes: S_T = Total settlement (Table 6); S_{V1D} = Average vertical settlement due to volumetric compression using Boulanger and Idriss (2014) (BI-2014), Zhang et al. (2002) (ZRB-2002) procedures and de Greef and Lengkeek (2018) thin-layer correction; $S_{E,L}$ = Ejecta-induced settlement as the difference between the LiDAR-based S_T and S_{V1D}.

Note 3: The uncertainty for volumetric settlement was derived based on the sensitivity of volumetric settlement to PGA, C_{FC}, and P_L for each earthquake event for VsVp 57203 *Shirley Intermediate School* and CC LIQ 1 – CPT 5586 – *Vivian St* sites. Taking the 50th percentile as the baseline case, the minimum and maximum values corresponding to the difference between the 25th percentile and the 50th percentile and the 75th percentile and the 50th percentile were determined. The arithmetic mean of the range of the minimum and maximum difference was evaluated for each patch at the two sites. The maximum arithmetic mean for each earthquake event was rounded to the nearest five and used as the uncertainty value. Accordingly, the 1-D volumetric settlement uncertainties of ±20, ±50, ±25, and ±50 mm for the Sep-10, Feb-11, Jun-11, and Dec-11 earthquake events, respectively, were used for all sites in this study.

Table 9a: Coverage area and height of ejecta estimates for Patch A (20- and 50-m buffers) using photographs.

Earthquake Event	$A_{E,thick}$ (m^2)	$H_{E,thick}$ (mm)	$A_{E,thin}$ (m^2)	$H_{E,thin}$ (mm)	A_T (m^2)
Sep-10	0	0	0	0	87.6
Feb-11	0	0	0	0	87.6
Jun-11	0	0	0	0	87.6
Dec-11	0	0	0	0	87.6

Notes: $A_{E,thick/thin}$ = Coverage area of thick/thin ejecta layers; $H_{E,thick/thin}$ = Lower-upper estimate of height of thick/thin ejecta layers; A_T = Total assessment area of a buffer being considered; Thin and thick layers correspond to light gray and dark gray colors of ejecta observed in aerial photographs.

Table 9b: Coverage area and height of ejecta estimates for Road (20-m buffer) using photographs.

EQ Event	$H_{E,prism/pyr}$ (mm)	$V_{E,prism+pyr}$ (m³)	$H_{E,thick1}$ (mm)	$A_{E,thick1}$ (m²)	$H_{E,thick2}$ (mm)	$A_{E,thick2}$ (m²)	$H_{E,thin}$ (mm)	$A_{E,thin}$ (m²)	A_T (m²)
Sep-10	0	0	0	0	0	0	0	0	430
Feb-11	28-200	7.6-10.9	0	0	0	0	5-10	271	430
Jun-11	22-150	6.1-9.9	0	0	0	0	5-10	228	418*
Dec-11	0	0	0	0	0	0	0	0	430

Notes: $H_{E,prism/pyr}$ = Lower-upper estimate of ejecta height near the curb based on 2-4% cross slope of normal crown; $V_{E,prism+pyr}$ = Lower-upper estimate of total volume of prismatic- and pyramidal-shape ejecta; $A_{E,thin/thick}$ = Coverage area of thin/thick ejecta layers; $H_{E,thin/thick}$ = Lower-upper estimate of height of thin/thick ejecta layers; A_T= Total assessment area of a buffer being considered; * indicates reduction in A_T due to the presence of shadows.

Table 9c: Coverage area and height of ejecta estimates for Road (50-m buffer) using photographs.

EQ Event	$H_{E,prism/pyr}$ (mm)	$V_{E,prism+pyr}$ (m³)	$H_{E,thick1}$ (mm)	$A_{E,thick1}$ (m²)	$H_{E,thick2}$ (mm)	$A_{E,thick2}$ (m²)	$H_{E,thin}$ (mm)	$A_{E,thin}$ (m²)	A_T (m²)
Sep-10	0	0	0	0	0	0	0	0	1102
Feb-11	22-200	22.4-32.8	60-120	53.4	40-60	10.8	5-10	576	1102
Jun-11	22-150	22.2-34.8	0	0	0	0	5-10	497	1067*
Dec-11	0	0	0	0	0	0	0	0	1102

Notes: $H_{E,prism/pyr}$ = Lower-upper estimate of ejecta height near the curb based on 2-4% cross slope of normal crown; $V_{E,prism+pyr}$ = Lower-upper estimate of total volume of prismatic- and pyramidal-shape ejecta; $A_{E,thin/thick}$ = Coverage area of thin/thick ejecta layers; $H_{E,thin/thick}$ = Lower-upper estimate of height of thin/thick ejecta layers; A_T= Total assessment area of a buffer being considered; * indicates reduction in A_T due to the presence of shadows.

Note 4: The values in Table 9 correspond to the coverage area of ejecta outlined in aerial photographs (Figures 29, 33, 65, and 66) and the lower and upper estimates of ejecta height based on geometrical approximations, ground photographs (Figure 67), and EQC LDAT property inspection reports. The ejecta-induced settlement using photographs and engineering judgment, $S_{E,P}$, is estimated as

$$S_{E,P} = \frac{\sum_{i=1}^{a} A_{E,thick,i} * H_{E,thick,i} + \sum_{j=1}^{b} A_{E,thin,j} * H_{E,thin,j}}{A_T} + \frac{\frac{1}{2}\sum_{n=1}^{f} W_{E,prism,n} * H_{E,prism,n} * L_{E,prism,n}}{A_T} + \frac{\frac{1}{6}\sum_{p=1}^{g} W_{E,pyramid,p} * H_{E,pyramid} * L_{E,pyramid}}{A_T} = \frac{\sum_{i=1}^{a} V_{E,thick,i} + \sum_{j=1}^{b} V_{E,thin,j} + \sum_{n=1}^{f} V_{E,prism,n} + \sum_{p=1}^{g} V_{E,pyramid,p}}{A_T}$$

where

- $A_{E,thick,i}$ and $H_{E,thick,i}$ are the area and the height of a thick ejecta layer, respectively;

- $A_{E,thin,j}$ and $H_{E,thin,j}$ are the area and the height of a thin ejecta layer, respectively;
- $W_{E,prism,n}$ and $L_{E,prism,n}$ are the width and the length of the coverage area of a prismatically shaped ejecta layer, respectively, and $H_{E,prism,n}$ is the height of a prism-like ejecta layer;
- $W_{E,pyr,p}$ and $L_{E,pyr,p}$ are the width and the length of the coverage area of a pyramid-like ejecta layer, respectively, and $H_{E,pyr,p}$ is the height of a pyramid-like ejecta layer;
- A_T is the total assessment area for a buffer being considered (Figure 1).

Table 10: Ejecta-induced settlement estimates for Patch A and Road based on photographs.

Earthquake Event	Patch A (20- and 50-m buffers)		Road (20-m buffer)		Road (50-m buffer)	
	$S_{E,P,lower}$ (mm)	$S_{E,P,upper}$ (mm)	$S_{E,P,lower}$ (mm)	$S_{E,P,upper}$ (mm)	$S_{E,P,lower}$ (mm)	$S_{E,P,upper}$ (mm)
Sep-10	0	0	0	0	0	0
Feb-11	0	0	21	32	26	41
Jun-11	0	0	17	29	23	37
Dec-11	0	0	0	0	0	0

Note: $S_{E,P,lower}$ and $S_{E,P,upper}$ correspond to lower and upper estimates of $S_{E,P}$, respectively.

Table 11: Best final estimates of ejecta-induced settlement for Patch A and Road.

EQ Event	Patch A (20- and 50-m buffers)			Road (20-m buffer)			Road (50-m buffer)		
	$S_{E,L}$ (mm)	$S_{E,P}$ (mm)	$S_{E,final}$ (mm)	$S_{E,L}$ (mm)	$S_{E,P}$ (mm)	$S_{E,final}$ (mm)	$S_{E,L}$ (mm)	$S_{E,P}$ (mm)	$S_{E,final}$ (mm)
Sep-10	ND	0	0	ND	0	0	ND	0	0
Feb-11	ND	0	0	23±71	27±5	25±25	-5±71	34±7	35±5
Jun-11	ND	0	0	29±56	23±6	25±20	32±56	30±7	30±20
Dec-11	ND	0	0	ND	0	0	ND	0	0

Notes: $S_{E,L}$ = Ejecta-induced settlement based on LiDAR data reported in Table 8; $S_{E,P}$ = Median ejecta-induced settlement for the range of values reported in Table 10; $S_{E,final}$ = Best final estimate of ejecta-induced settlement rounded to the nearest 5; Final plus/minus values are also rounded to the nearest 5; ND = Not determined.

Note 5:

- Patch A: $S_{E,final}$ is based solely on $S_{E,P}$ for all earthquake events due to the evident absence of ejecta (also confirmed by the LDAT property inspection report).
- Road (20-m buffer): $S_{E,final}$ for the Sep-10 and Dec-11 EQs is equal to $S_{E,P}$ due to the evident absence of ejecta. $S_{E,final}$ for the Feb-11 and Jun-11 EQs is a weighted average of $S_{E,L}$ and $S_{E,P}$ with weights of 1/3 and 2/3, respectively. The uncertainty associated with $S_{E,final}$ for the Feb-11 and Jun-11 EQs is also a weighted average of uncertainties associated with $S_{E,L}$ and $S_{E,P}$ with the same weights of 1/3 and 2/3, respectively.
- Road (50-m buffer): $S_{E,final}$ for the Sep-10, Feb-11, and Dec-11 EQs is equal to $S_{E,P}$ due to the evident absence of ejecta for the Sep-10 and Dec-11 EQs and the negative $S_{E,L}$ value for the Feb-11 EQ. $S_{E,final}$ for the Jun-11 EQ is a weighted average of $S_{E,L}$ and $S_{E,P}$ with weights of 1/3

and 2/3, respectively. The uncertainty associated with $S_{E,final}$ for the Jun-11 EQ is also a weighted average of uncertainties associated with $S_{E,L}$ and $S_{E,P}$ with the same weights of 1/3 and 2/3, respectively.

- The weight coefficients are based on the LiDAR error bands, LPI prediction error (Maurer et al. 2014[3]), presence of ejecta at the time of LiDAR surveys, and completeness of visual evidence (i.e., ground and aerial photographs and EQC LDAT property inspection reports for the site). The Shortland St site is not in the apparent zone of higher or lower ground surface subsidence for the Sep-10 or Feb-11 EQ. The site is in the zone of slight to moderate LPI overprediction of liquefaction severity for the Sep-10 and Feb-11 EQs. The LDAT property inspection report is available for Patch A; ejecta were not observed (Figure 67). Ejecta were not typically present at the properties within the 50-m buffer. There are no ground photographs of the road.

<u>Summary 1</u>:

- **The best estimate of the ejecta-induced free-field ground settlement at the Shortland St site for the SEP 2010, FEB 2011, JUN 2011, and DEC 2011 earthquake is 0 mm, 0 mm, 0 mm, and 0 mm, respectively.**
- **The best estimate of the ejecta-induced free-field ground settlement of the road at the Shortland St site for the SEP 2010, FEB 2011, JUN 2011, and DEC 2011 earthquake is 0 mm, 25±25 mm, 25±20 mm, and 0 mm, respectively.**
- **Patch A ground (and ground at several other properties) is elevated relative to the road and retained by a 0.5-m high wall (Figures 8, 9, and 67). Thus, the ejecta-induced settlement of the road is more representative of the site.**

---

[3] Maurer, B. W., Green, R. A., Cubrinovski, M., & Bradley, B. A. (2014). Evaluation of the Liquefaction Potential Index for Assessing Liquefaction Hazard in Christchurch, New Zealand. *Journal of Geotechnical and Geoenvironmental Engineering*, 140(7), 04014032-1-11. doi:10.1061/(asce)gt.1943-5606.0001117

Figure 5: Location of the site.

Figure 6: Position of the site relative to nearby free-face features.

Figure 7: Position of the site relative to nearby buildings and vegetation.

Figure 8: Street view of the flat land.

Figure 9: Street view of the retained front lawns.

Figure 10: Satellite image of the site taken in Dec 2004.

Figure 11: Satellite image of the site taken in Mar 2009.

Figure 12: Satellite image of the site taken on Sep 3, 2010.

Figure 13: Satellite image of the site taken on Sep 5, 2010.

Figure 14: Satellite image of the site taken on Feb 7, 2011.

Figure 15: Satellite image of the site taken on Feb 23, 2011.

Figure 16: Satellite image of the site taken on Feb 26, 2011.

Figure 17: Satellite image of the site taken on Mar 8, 2011.

Figure 18: Satellite image of the site taken in Apr 2012.

Figure 19: Satellite image of the site taken in Jan 2013.

Figure 20: Satellite image of the site taken in Mar 2013.

Figure 21: Satellite image of the site taken in Sep 2013.

Figure 22: Satellite image of the site taken in Feb 2014.

Figure 23: Satellite image of the site taken in Aug 2014.

Figure 24: Satellite image of the site taken in Jan 2015.

Figure 25: Satellite image of the site taken in June 2015.

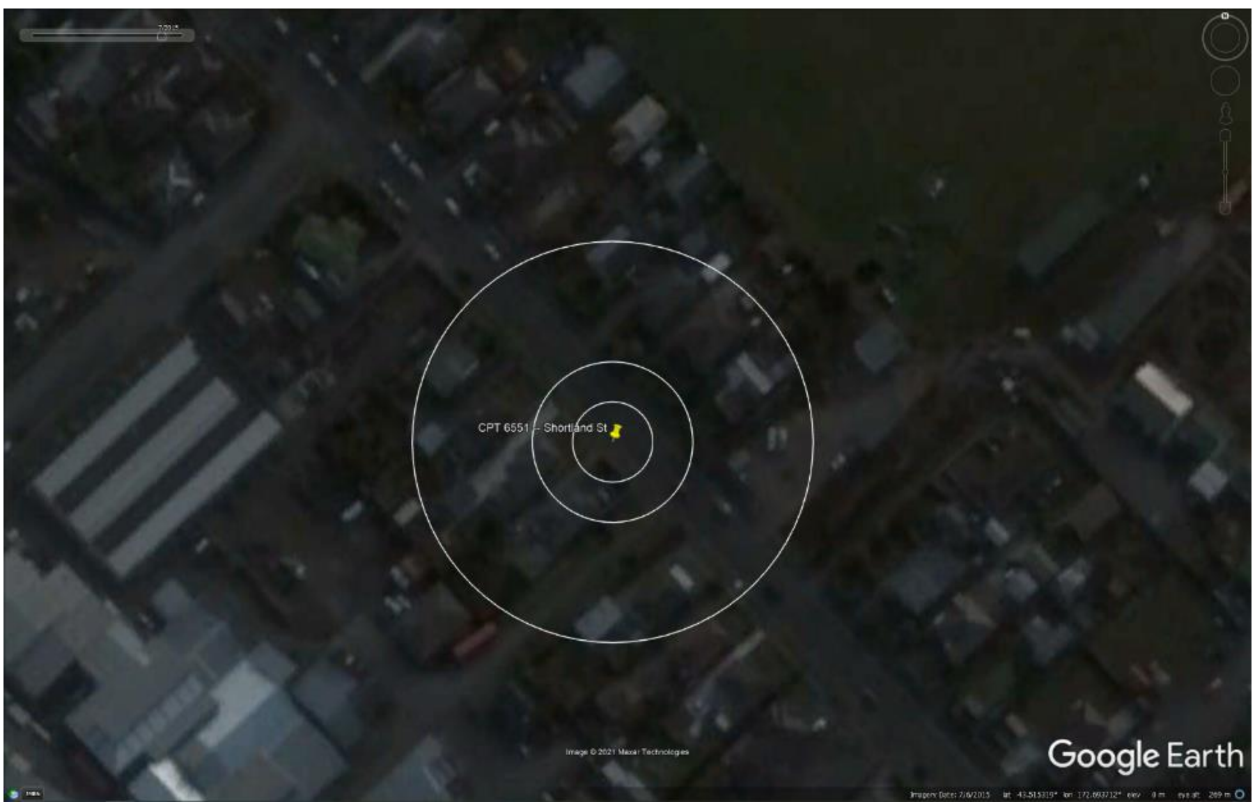

Figure 26: Satellite image of the site taken in July 2015.

Figure 27: Satellite image of the site taken in Sep 2015.

Figure 28: Satellite image of the site taken in Nov 2015.

Figure 29: Aerial photograph of the site taken on Sep 4, 2010.

Figure 30: Aerial photograph of the site taken on Feb 24, 2011.

Figure 31: No aerial photograph of the site was acquired on June 14-15, 2011.

Figure 32: Aerial photograph of the site taken on June 16, 2011.

Figure 33: Aerial photograph of the site taken on Dec 24, 2011.

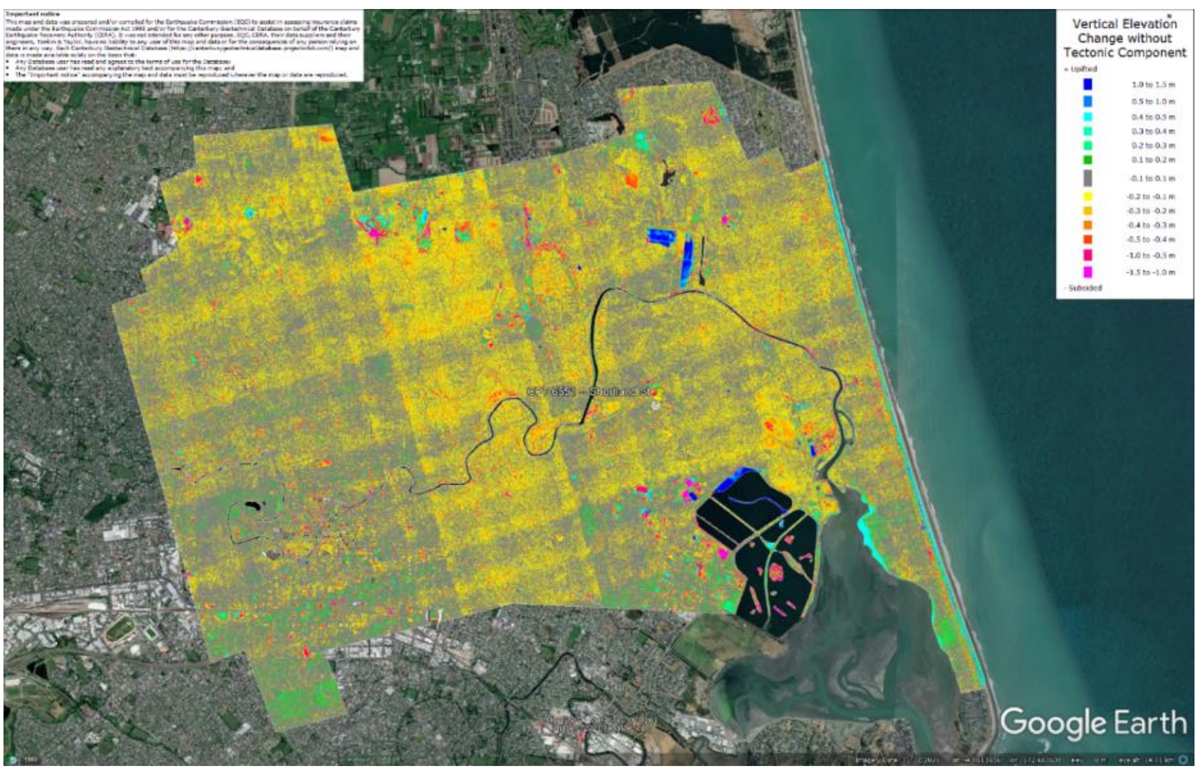

Figure 34: Vertical Ground Movements (Surface – Tectonic) for Sep 2010 Earthquake – the site is not in the apparent zone of overestimated or underestimated ground surface subsidence.

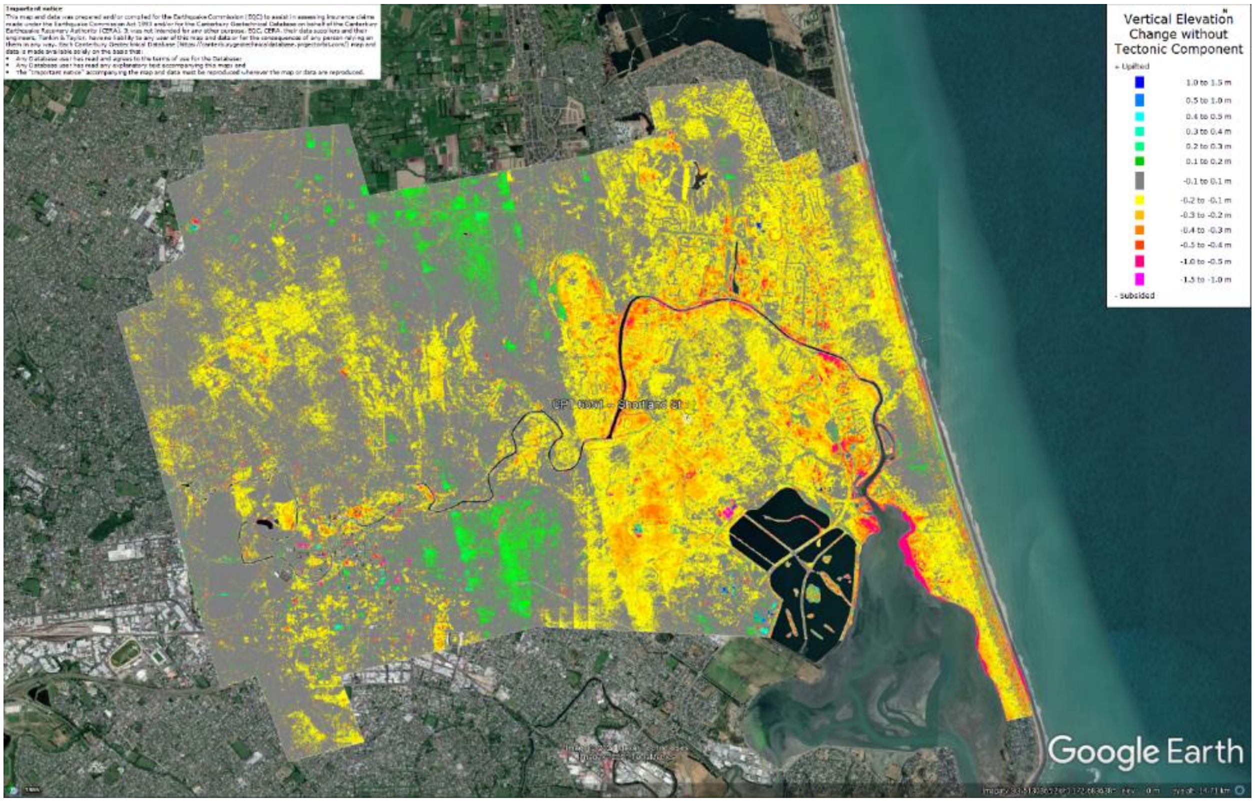

Figure 35: Vertical Ground Movements (Surface – Tectonic) for Feb 2011 Earthquake – the site is not in the apparent zone of overestimated or underestimated ground surface subsidence.

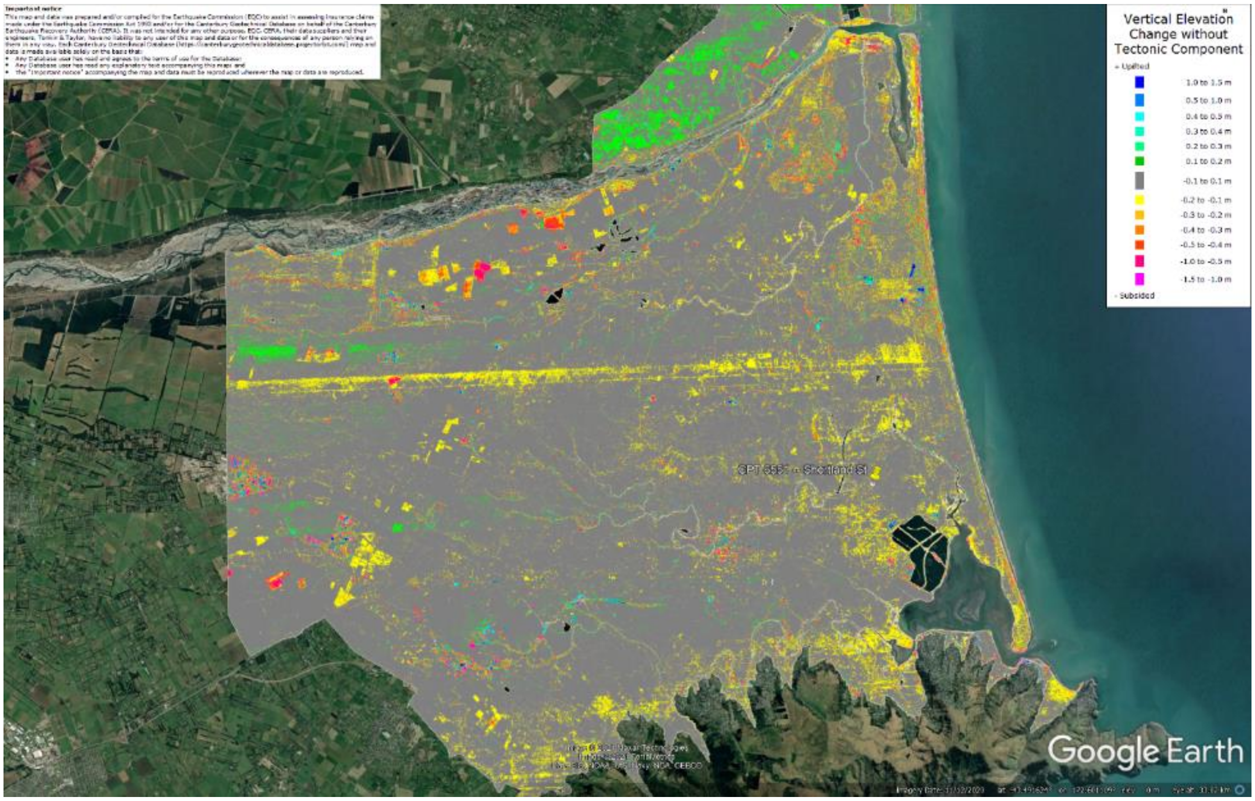

Figure 36: Vertical Ground Movements (Surface – Tectonic) for June 2011 Earthquake – the site is not in the apparent zone of overestimated or underestimated ground surface subsidence.

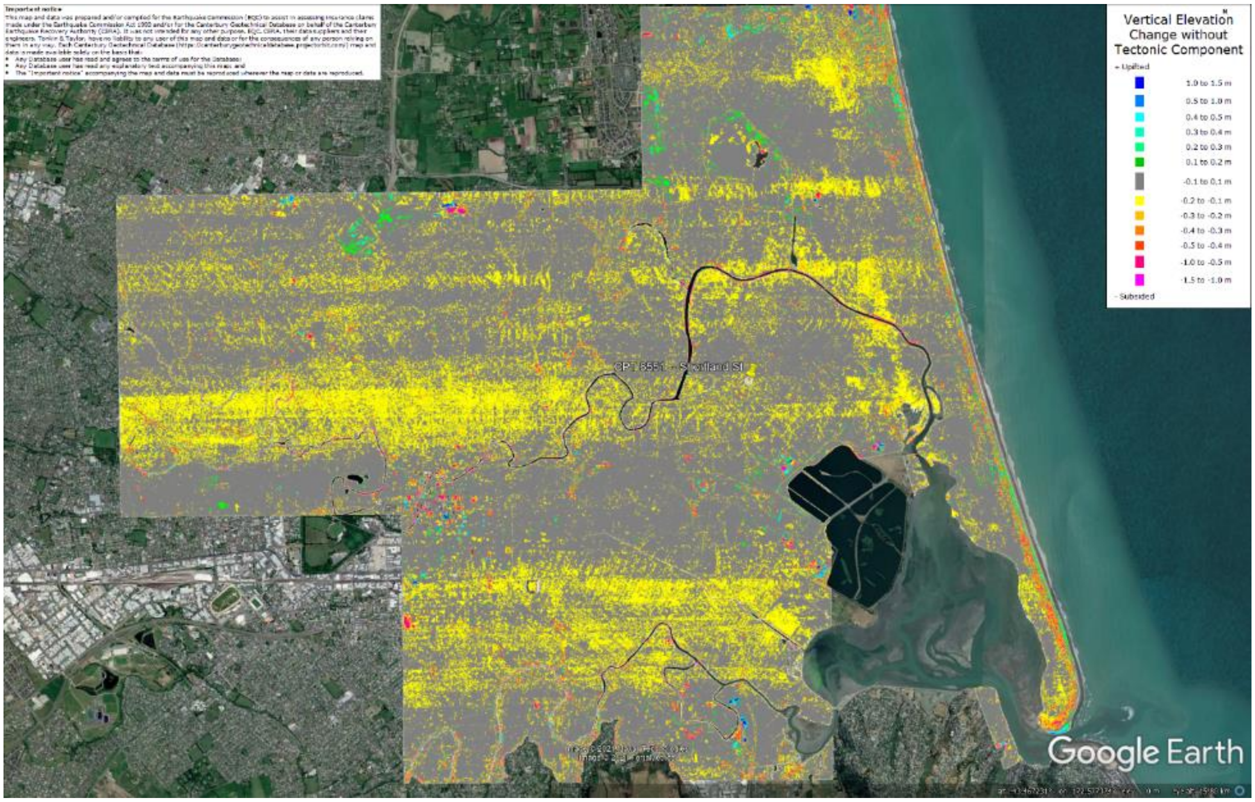

Figure 37: Vertical Ground Movements (Surface – Tectonic) for Dec 2011 Earthquake – the site is not in the apparent zone of overestimated ground surface subsidence (i.e., flight path error for Feb 2012 survey).

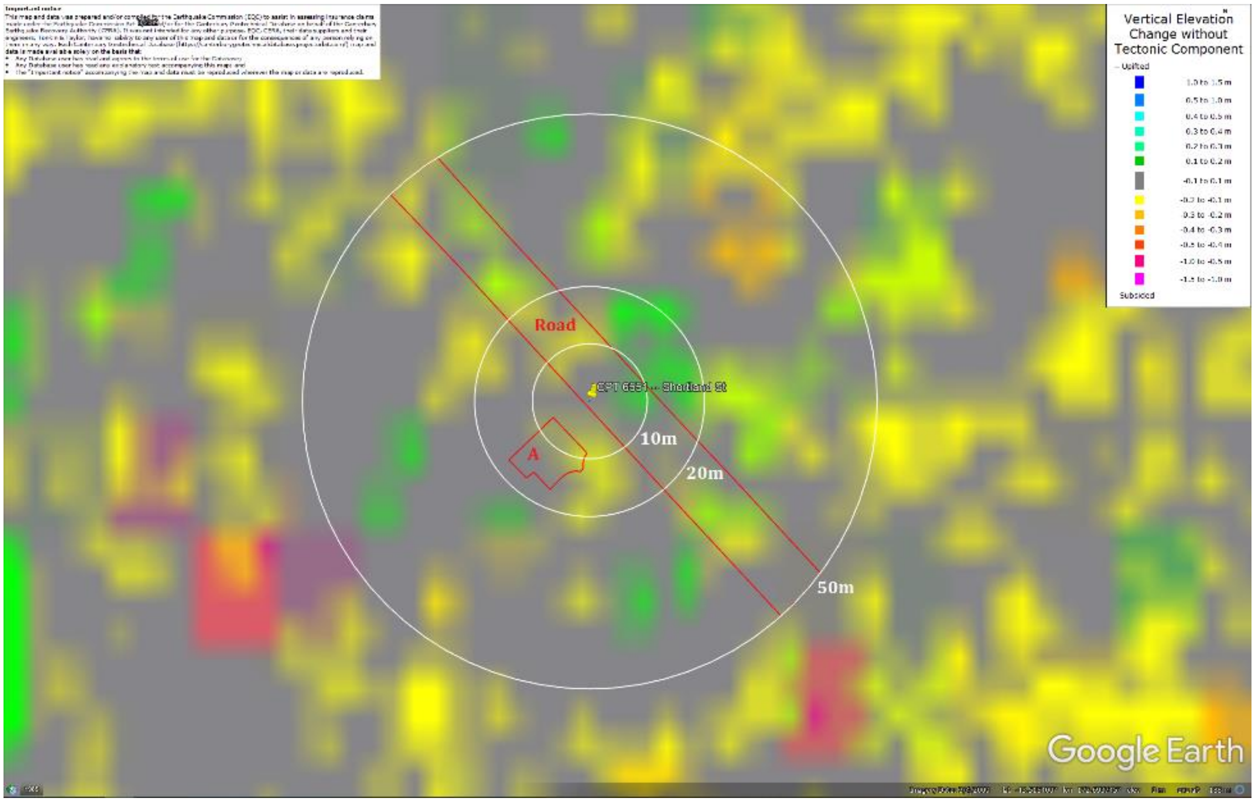

Figure 38: Ground surface subsidence without tectonic component for Sep 2010 Earthquake according to the LiDAR DEM.

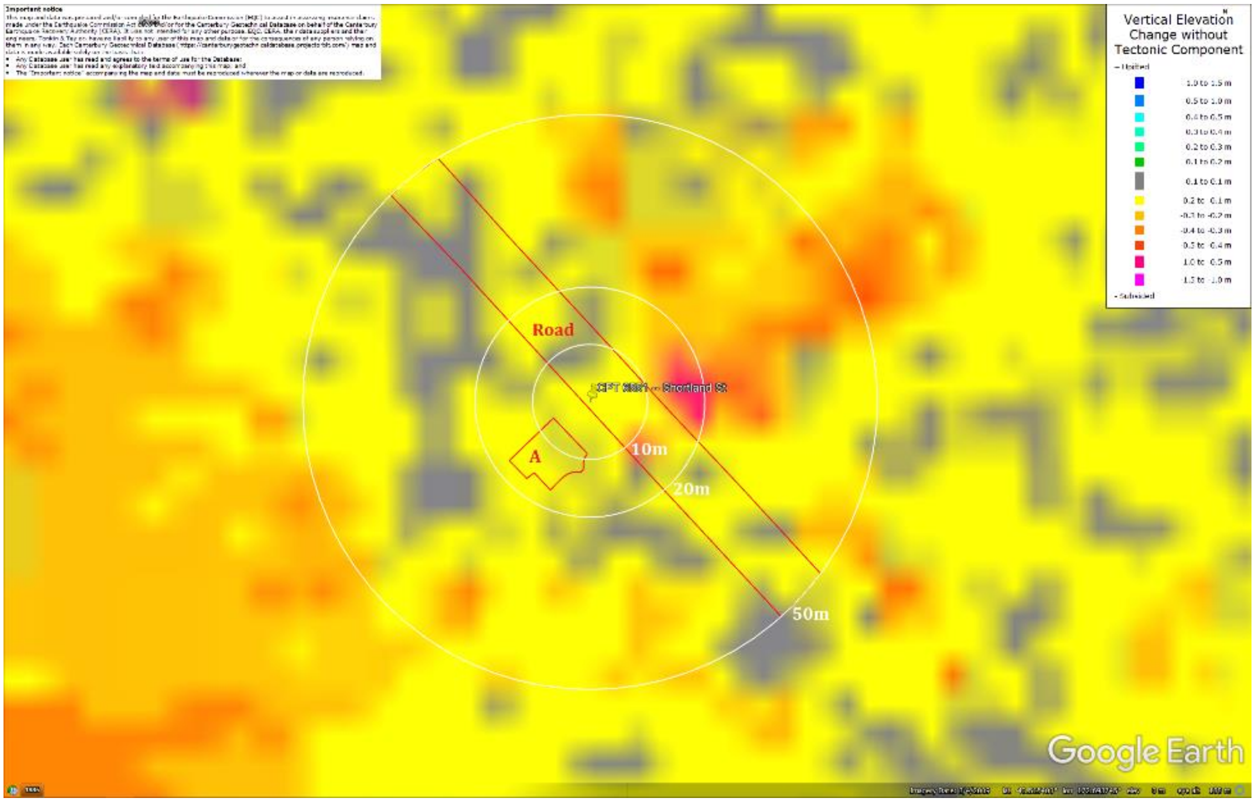

Figure 39: Ground surface subsidence without tectonic component for Feb 2011 Earthquake according to the LiDAR DEM.

Figure 40: Ground surface subsidence without tectonic component for June 2011 Earthquake according to the LiDAR DEM.

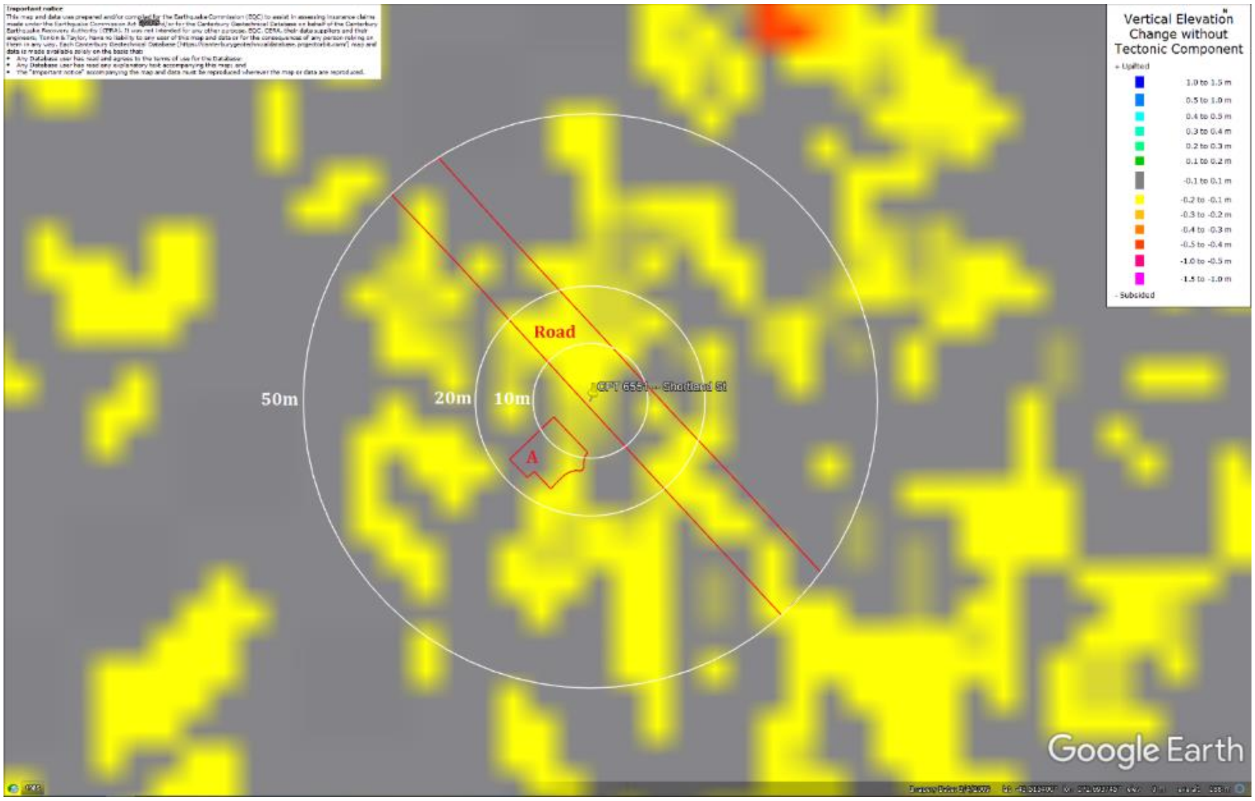

Figure 41: Ground surface subsidence without tectonic component for Dec 2011 Earthquake according to the LiDAR DEM.

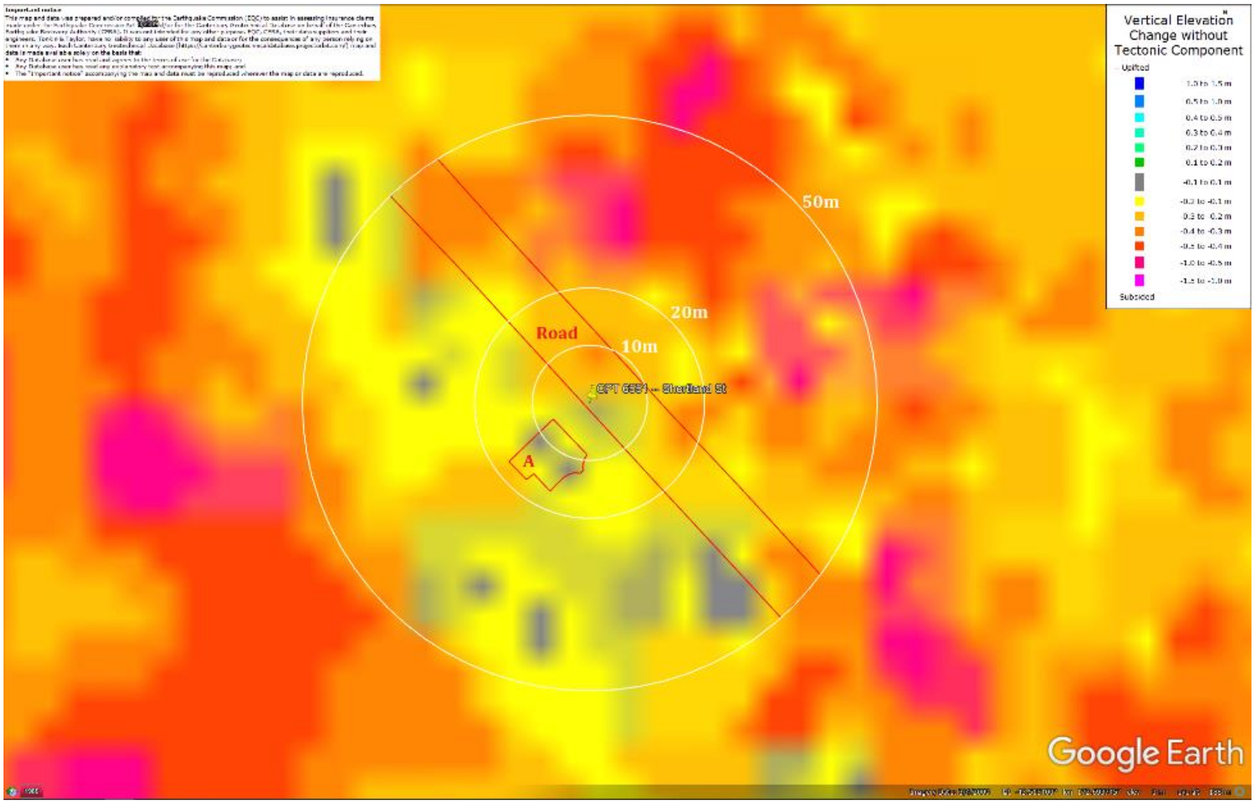

Figure 42: Ground surface subsidence without tectonic component for Canterbury Earthquake Sequence according to the LiDAR DEM.

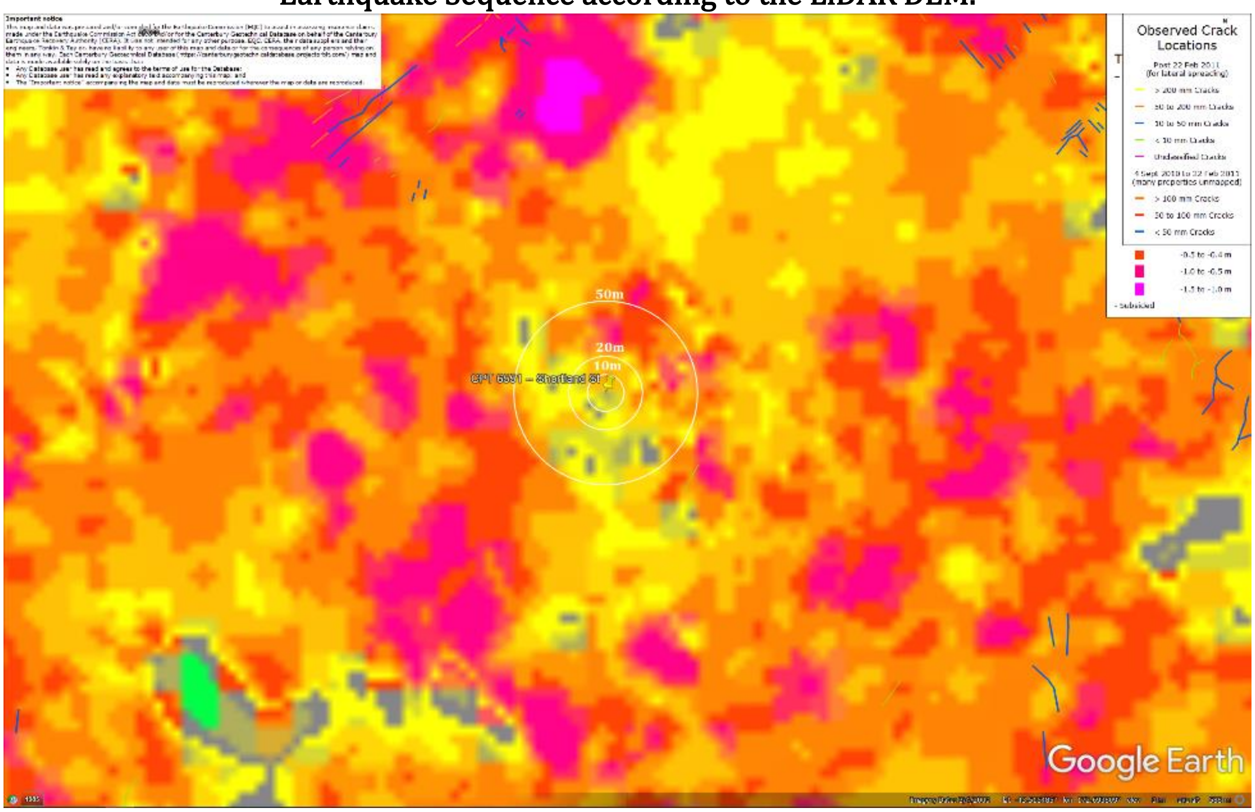

Figure 43: No lateral spreading for Canterbury Earthquake Sequence.

Figure 44: Vertical tectonic movements for Sep 2010 Earthquake.

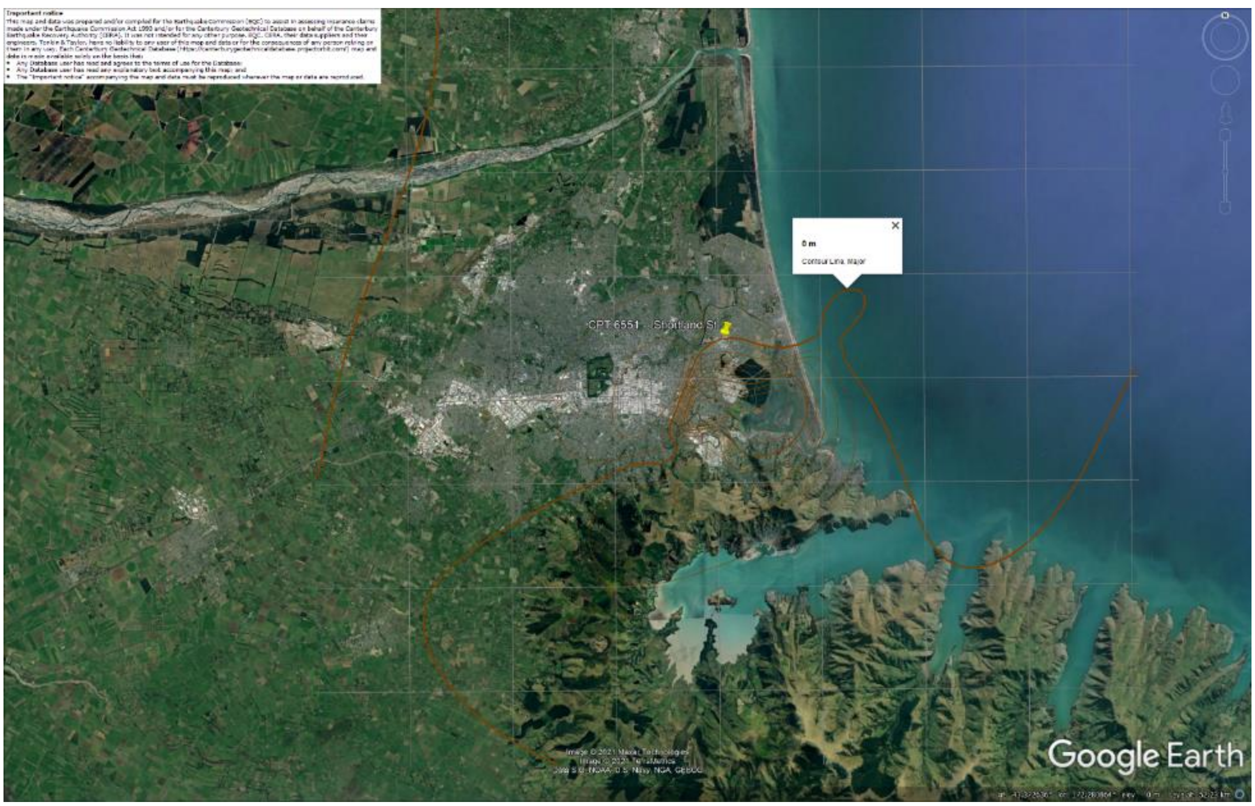

Figure 45: Vertical tectonic movements for Feb 2011 Earthquake.

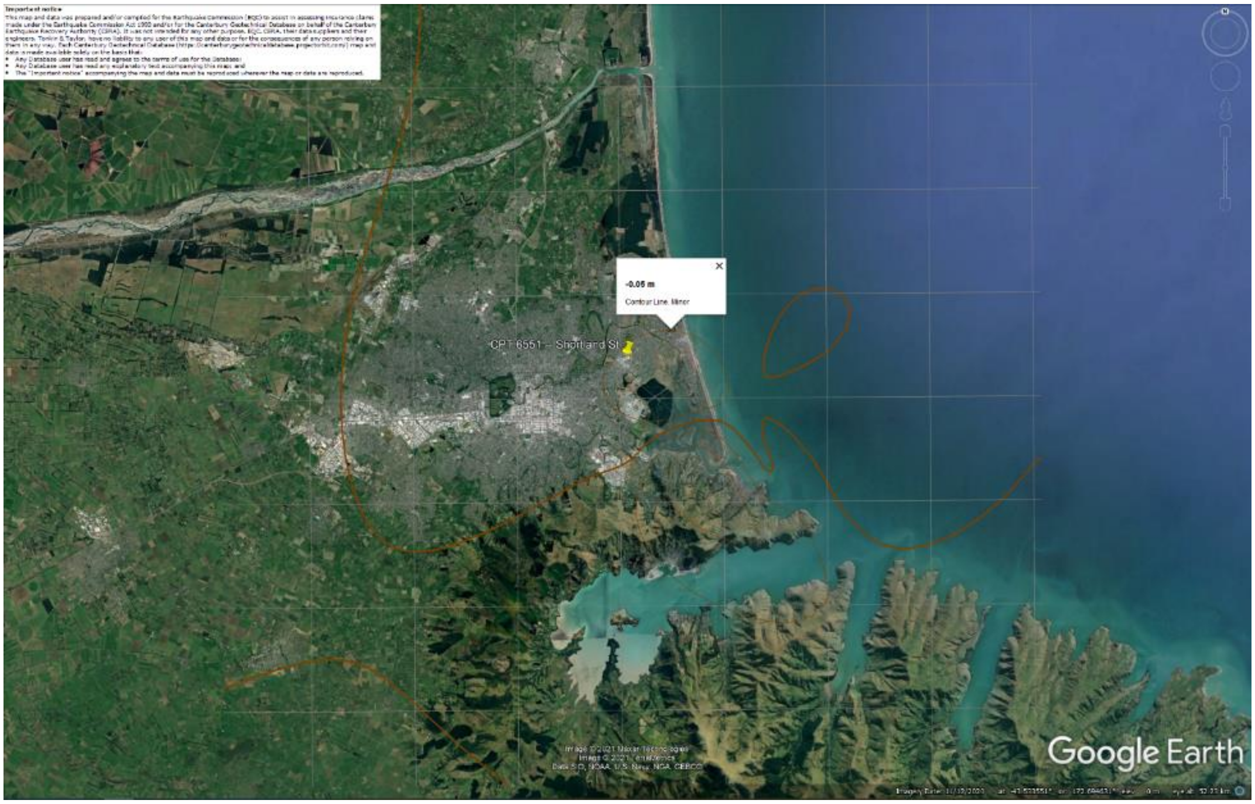

Figure 46: Vertical tectonic movements for June 2011 Earthquake.

Figure 47: Vertical tectonic movements for Dec 2011 Earthquake.

Figure 48: Vertical tectonic movements for Canterbury Earthquake Sequence.

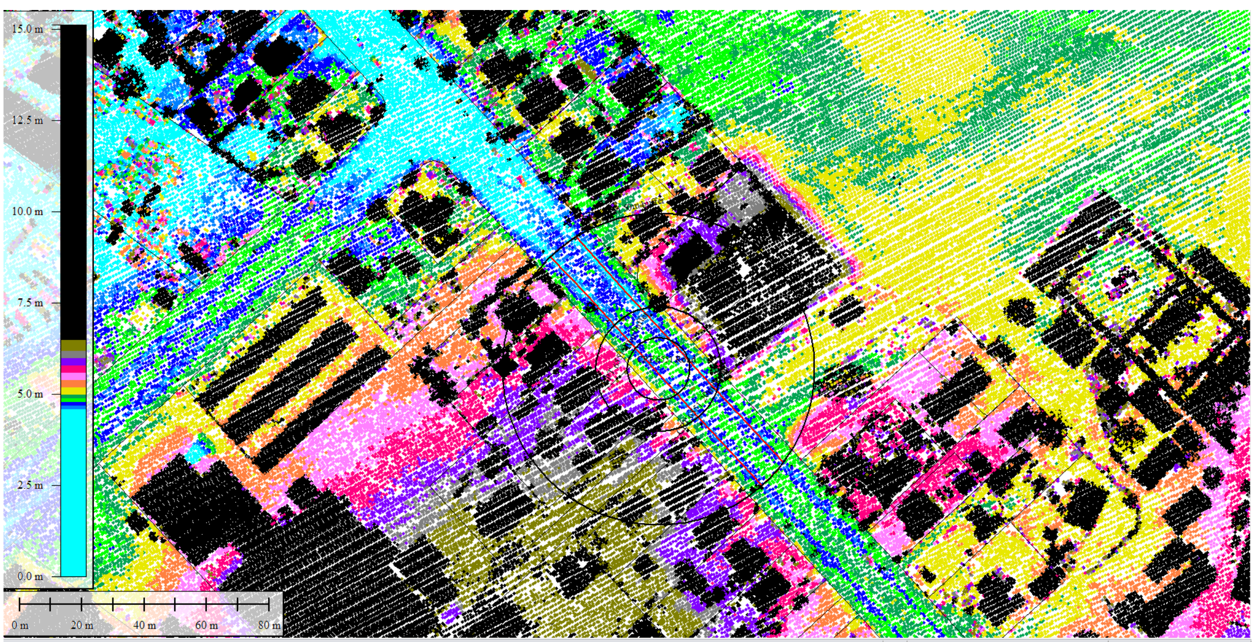

Figure 49: Sep 5, 2010 LiDAR survey.

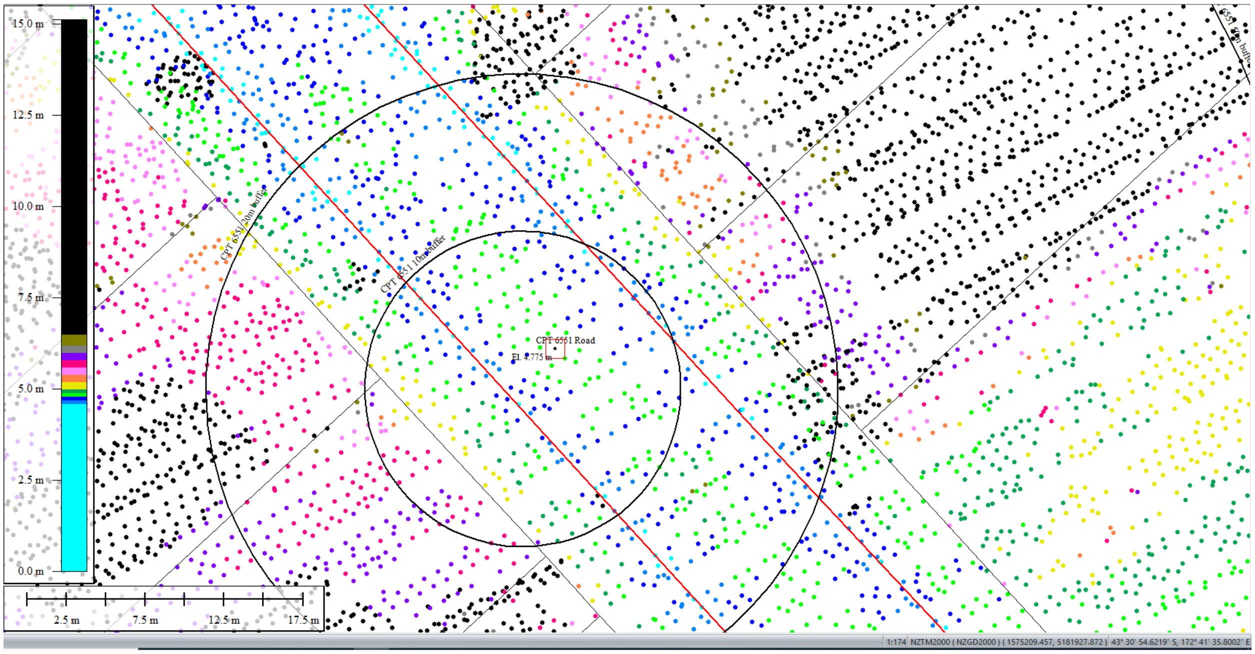

Figure 50: Ground surface elevation averaged over 10-m buffer for Road for Sep 5, 2010 LiDAR survey.

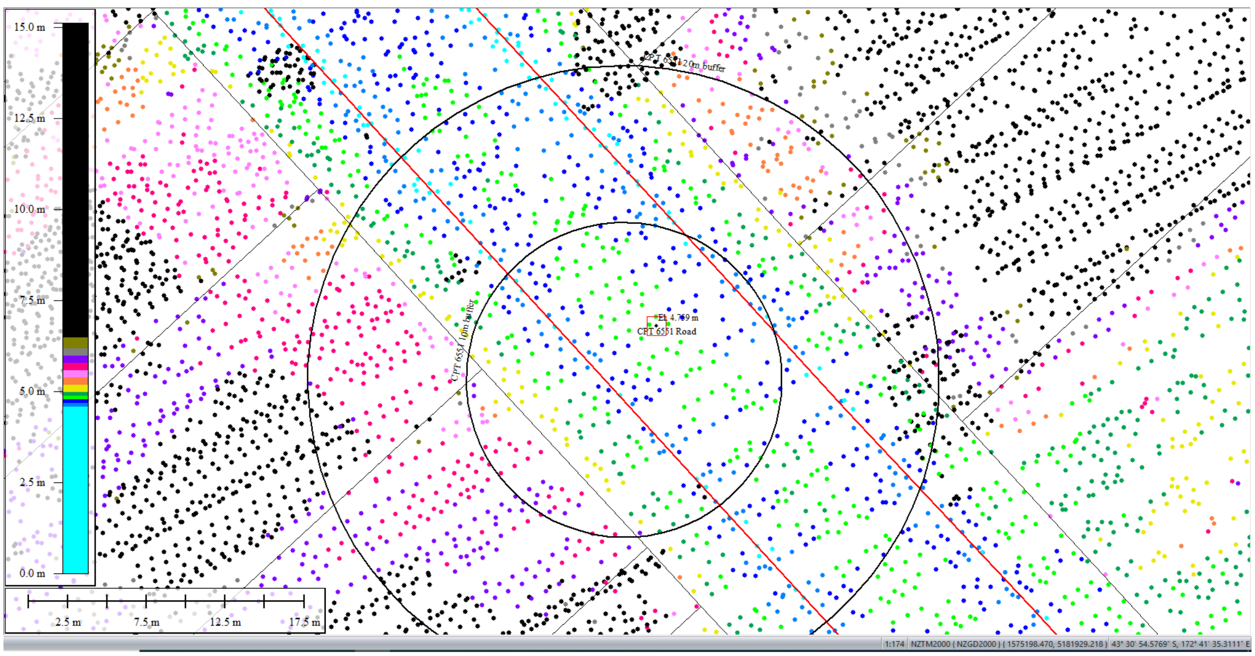

Figure 51: Ground surface elevation averaged over 20-m buffer for Road for Sep 5, 2010 LiDAR survey.

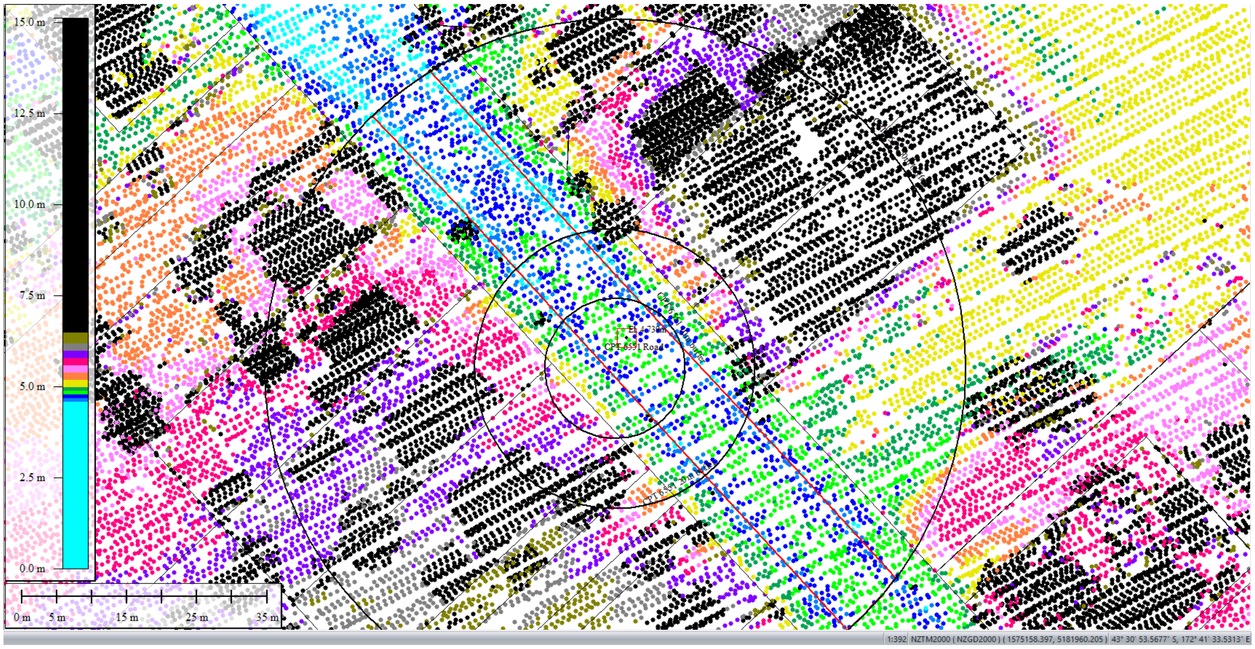

Figure 52: Ground surface elevation averaged over 50-m buffer for Road for Sep 5, 2010 LiDAR survey.

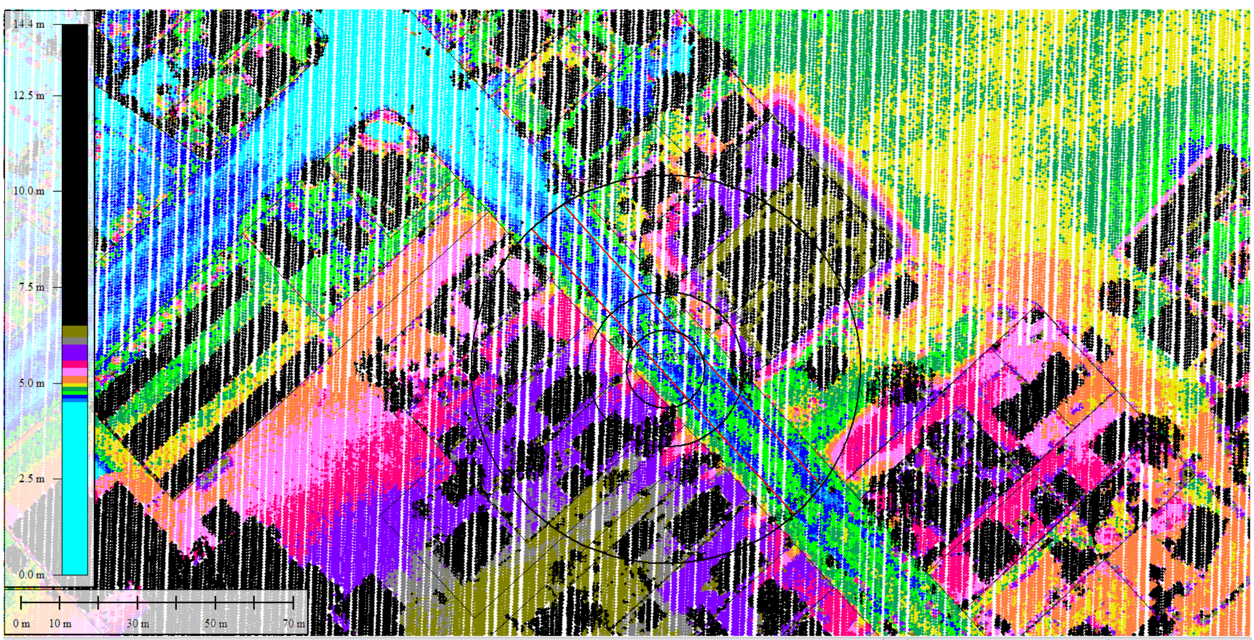

Figure 53: Mar 2011 LiDAR survey.

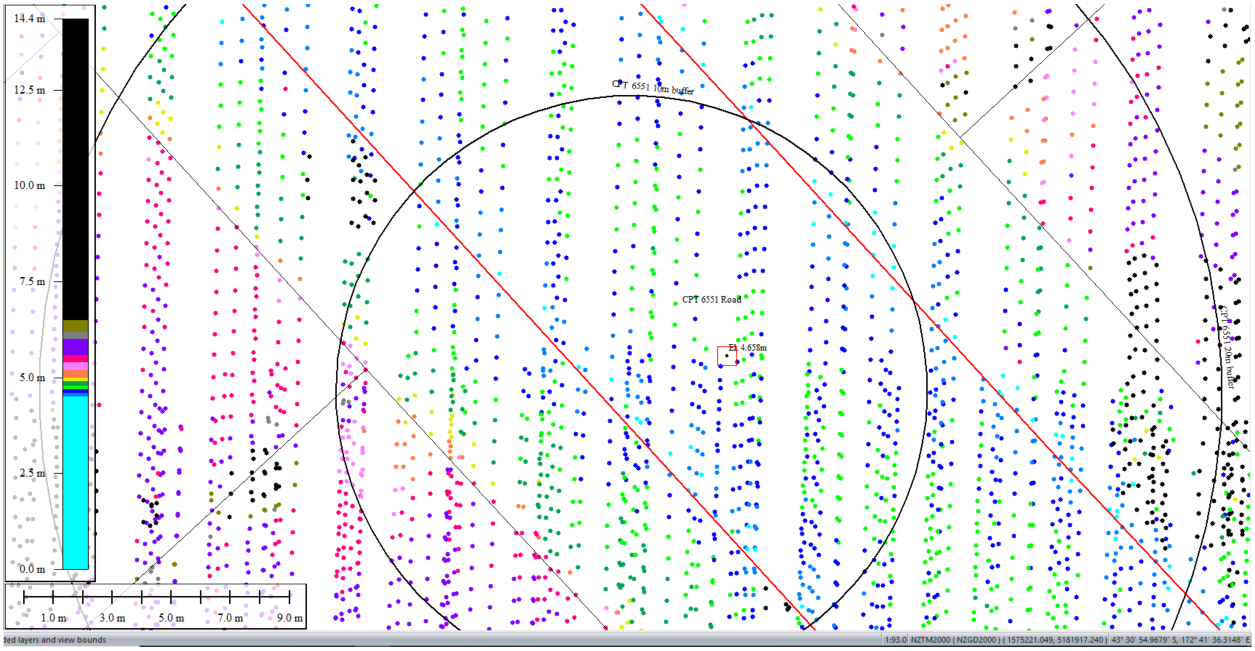

Figure 54: Ground surface elevation averaged over 10-m buffer for Road for Mar 2011 LiDAR survey.

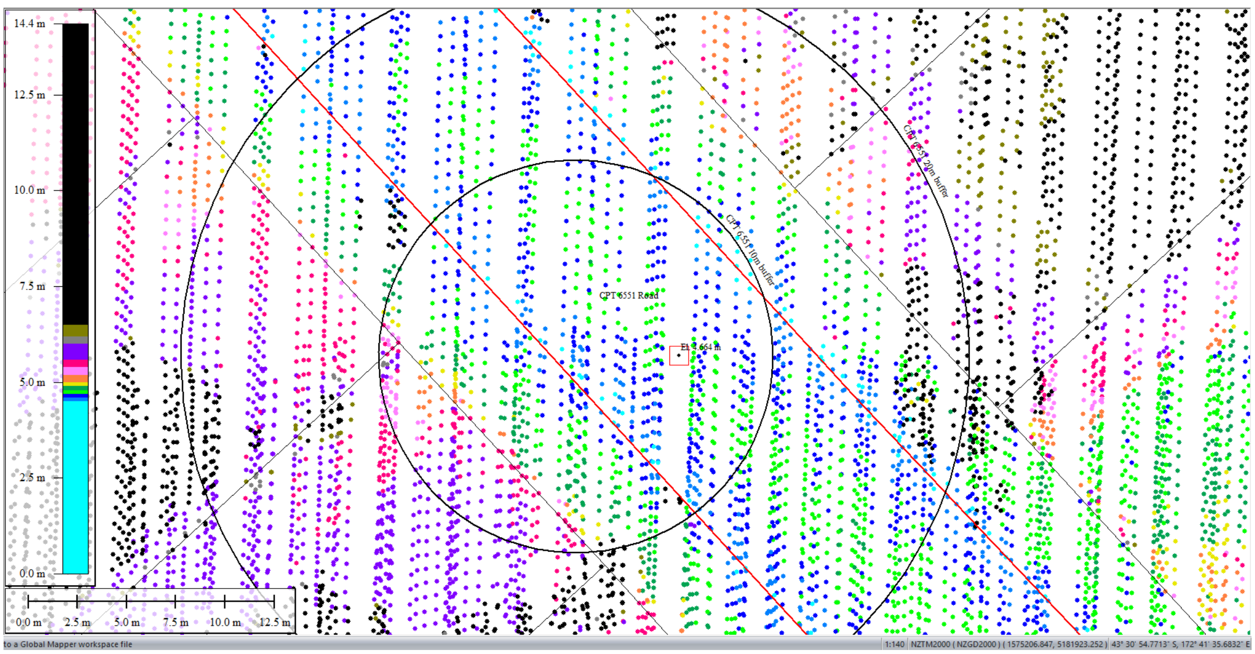

Figure 55: Ground surface elevation averaged over 20-m buffer for Road for Mar 2011 LiDAR survey.

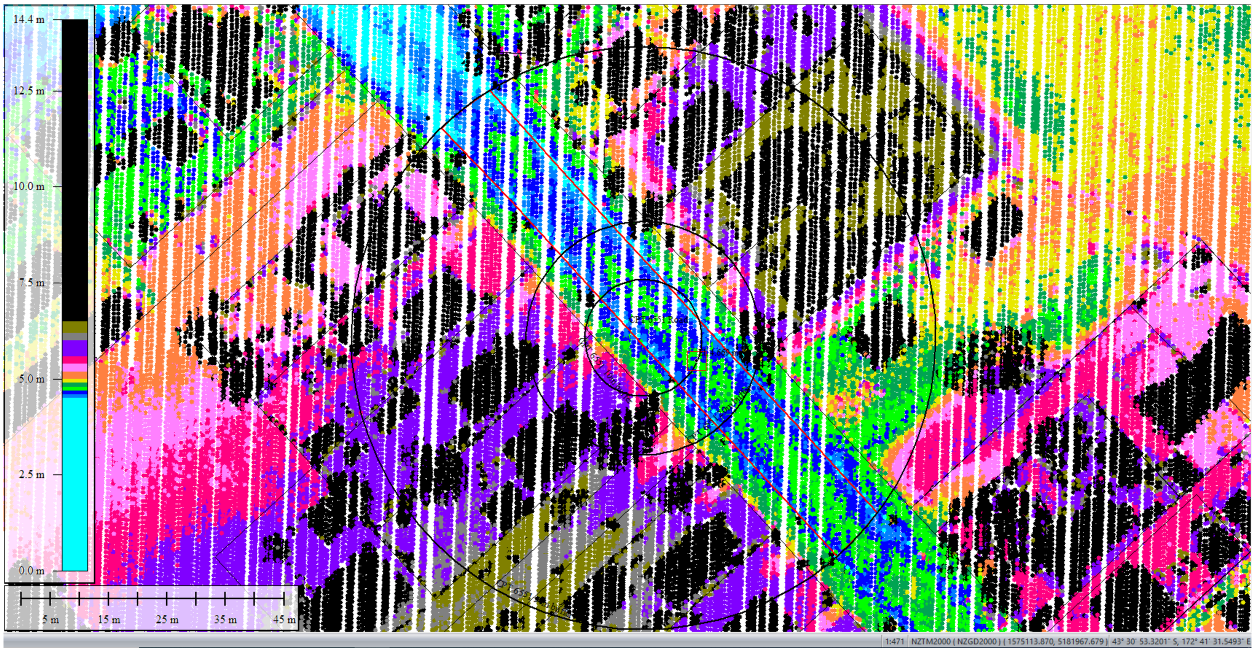

Figure 56: Ground surface elevation averaged over 50-m buffer for Road for Mar 2011 LiDAR survey.

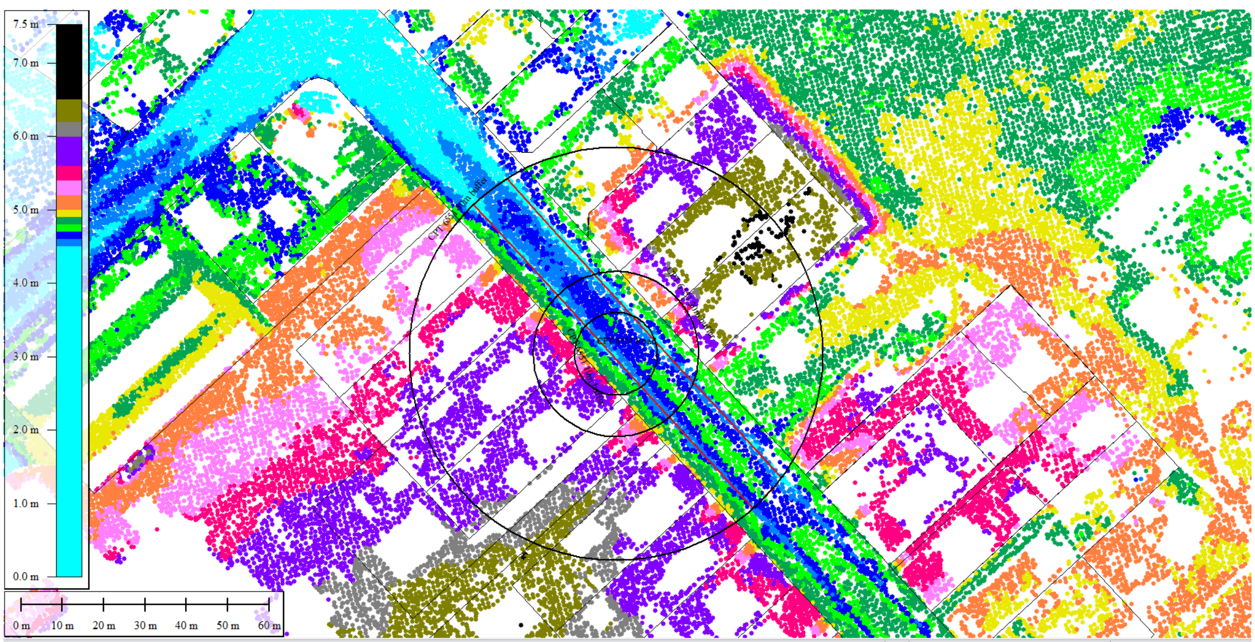

Figure 57: May 2011 LiDAR survey.

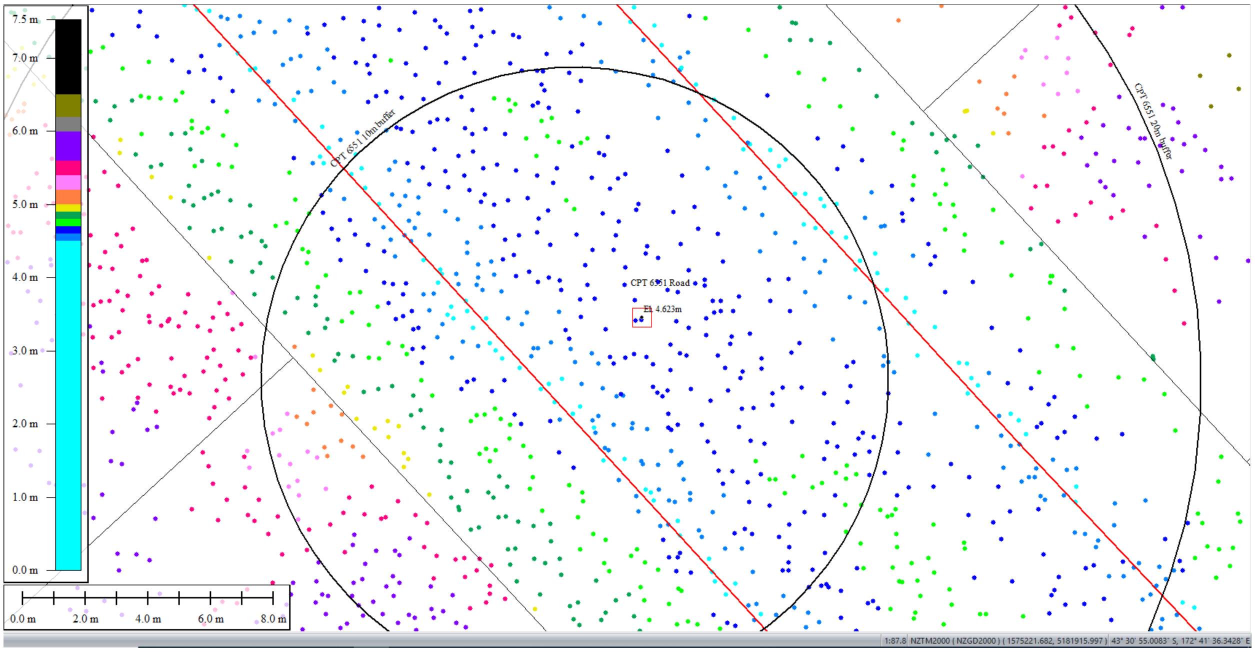

Figure 58: Ground surface elevation averaged over 10-m buffer for Road for May 2011 LiDAR survey.

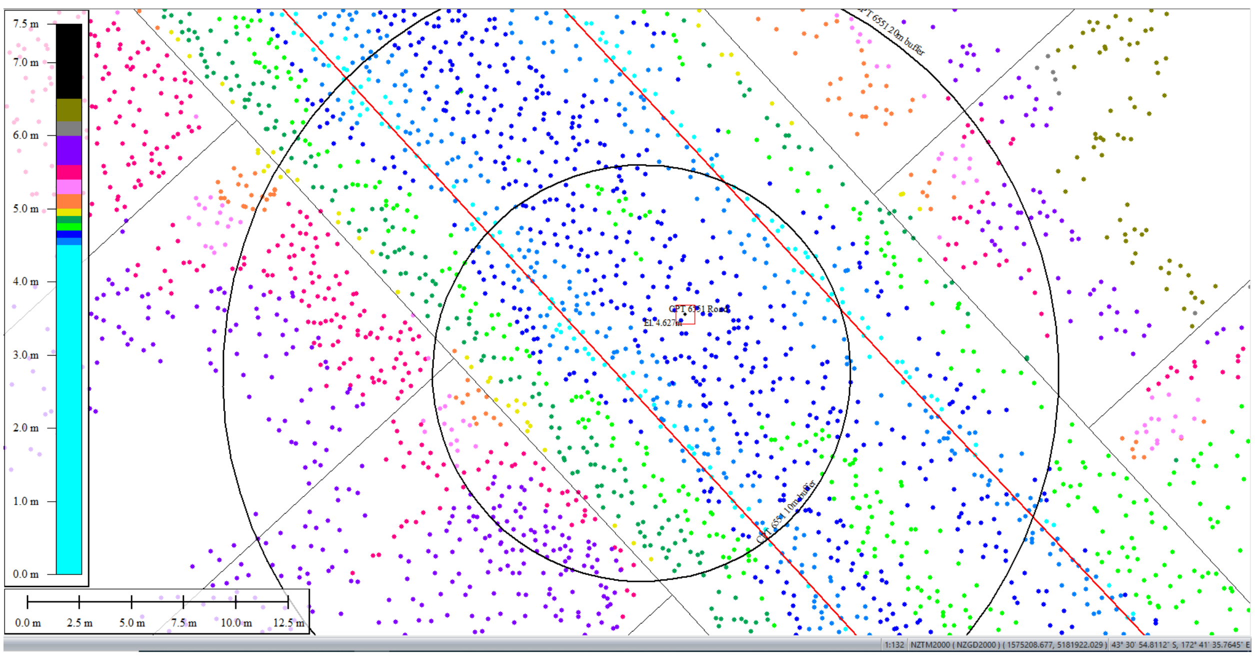

Figure 59: Ground surface elevation averaged over 20-m buffer for Road for May 2011 LiDAR survey.

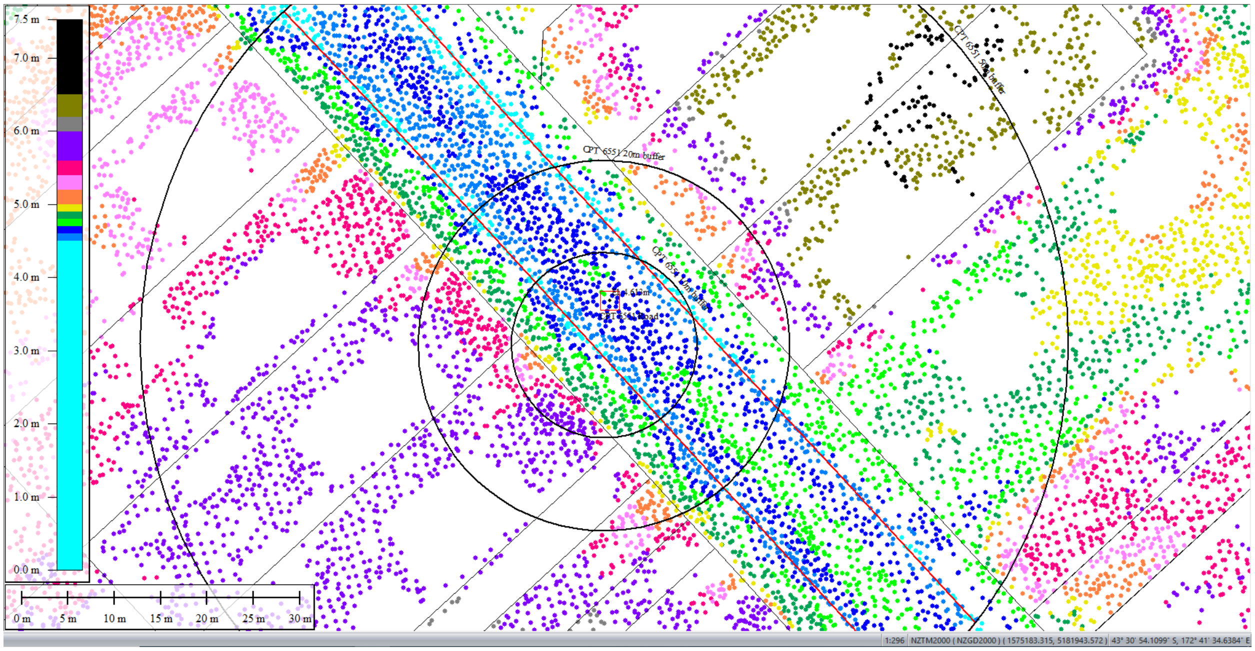

Figure 60: Ground surface elevation averaged over 50-m buffer for Road for May 2011 LiDAR survey.

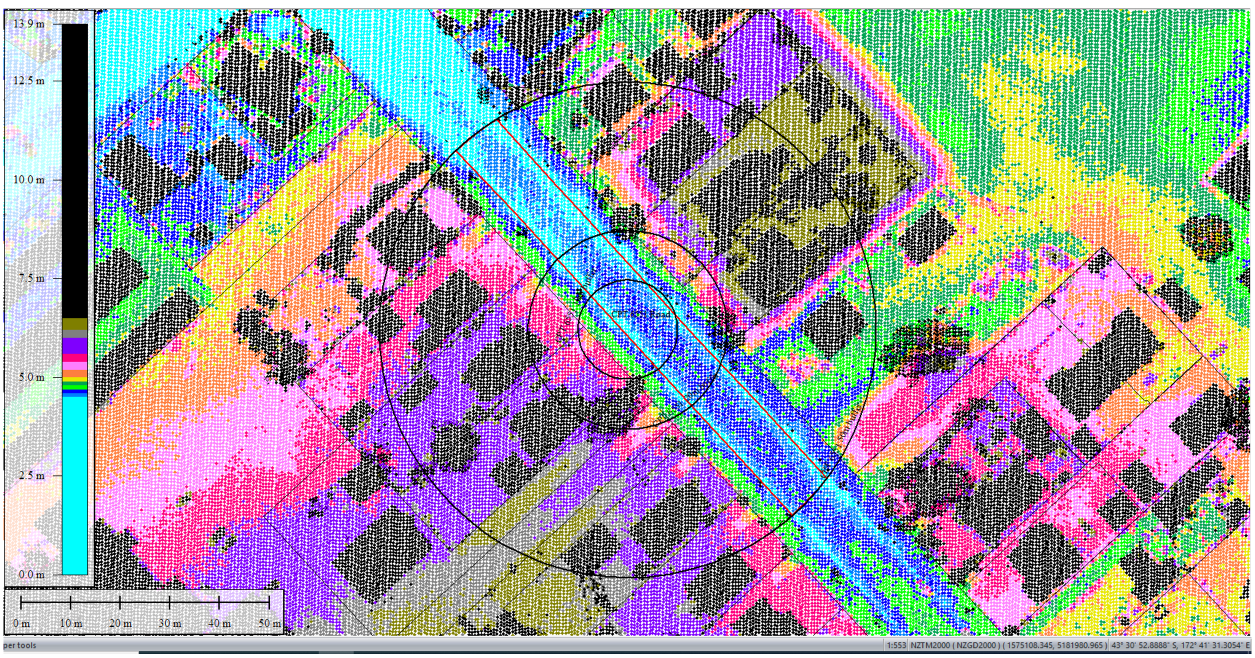

Figure 61: Sep 2011 LiDAR survey.

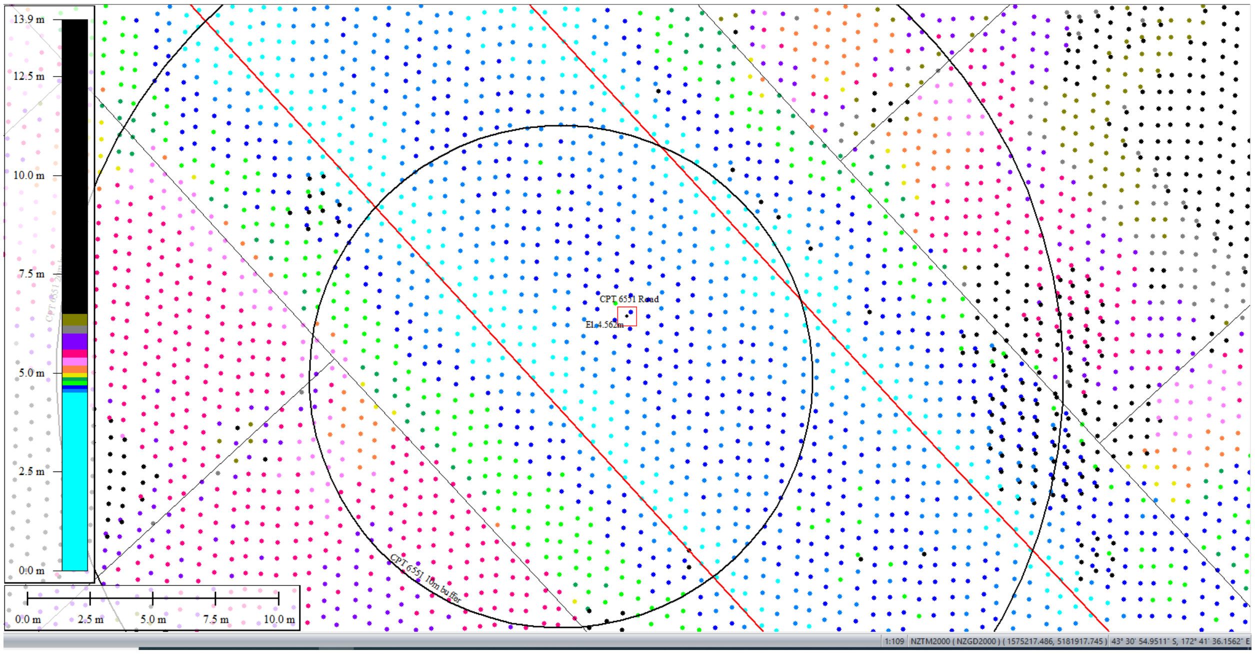

Figure 62: Ground surface elevation averaged over 10-m buffer for Road for Sep 2011 LiDAR survey.

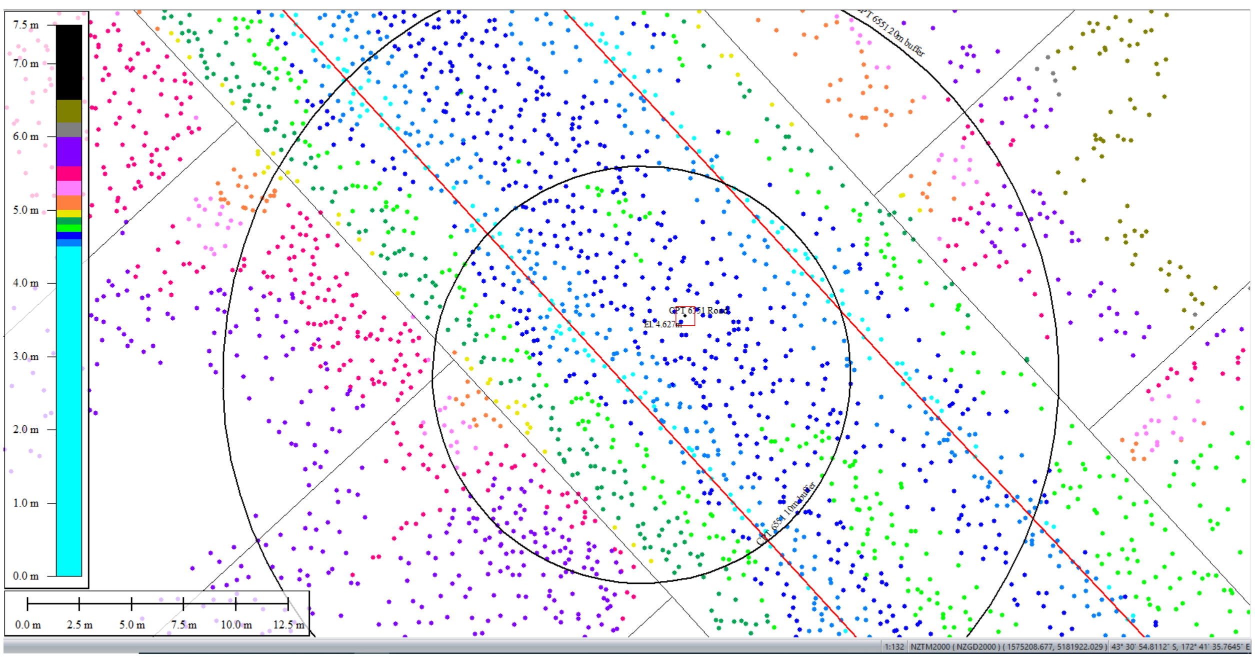

Figure 63: Ground surface elevation averaged over 20-m buffer for Road for Sep 2011 LiDAR survey.

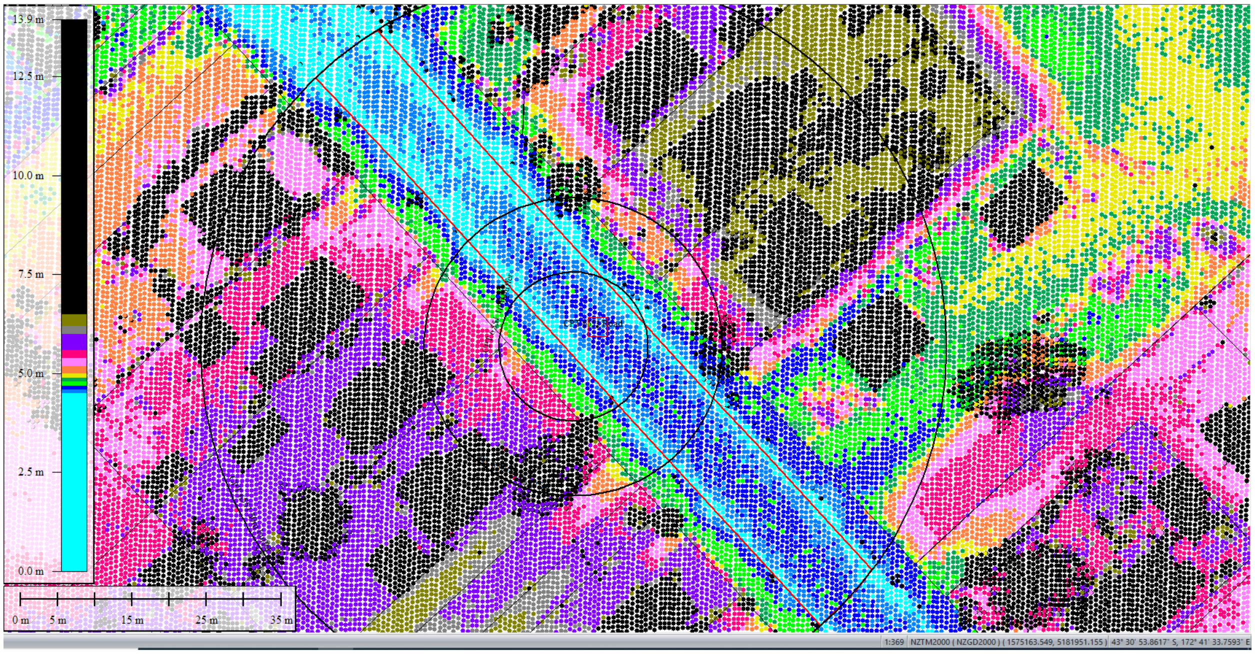

Figure 64: Ground surface elevation averaged over 50-m buffer for Road for Sep 2011 LiDAR survey (el. 4.547m).

Figure 65: Aerial photograph showing the ejecta outline at the site for Feb-11 EQ.

Figure 66: Aerial photograph acquired on 16 Jun 2011 showing the ejecta outline at the site for Jun-11 EQ.

Figure 67: Ground photograph showing absence of ejecta within Patch A (photograph date: Sep 2011).

Figure 68: PGA for Sep-10 EQ (st. dev. = 0.300-0.325 ln units).

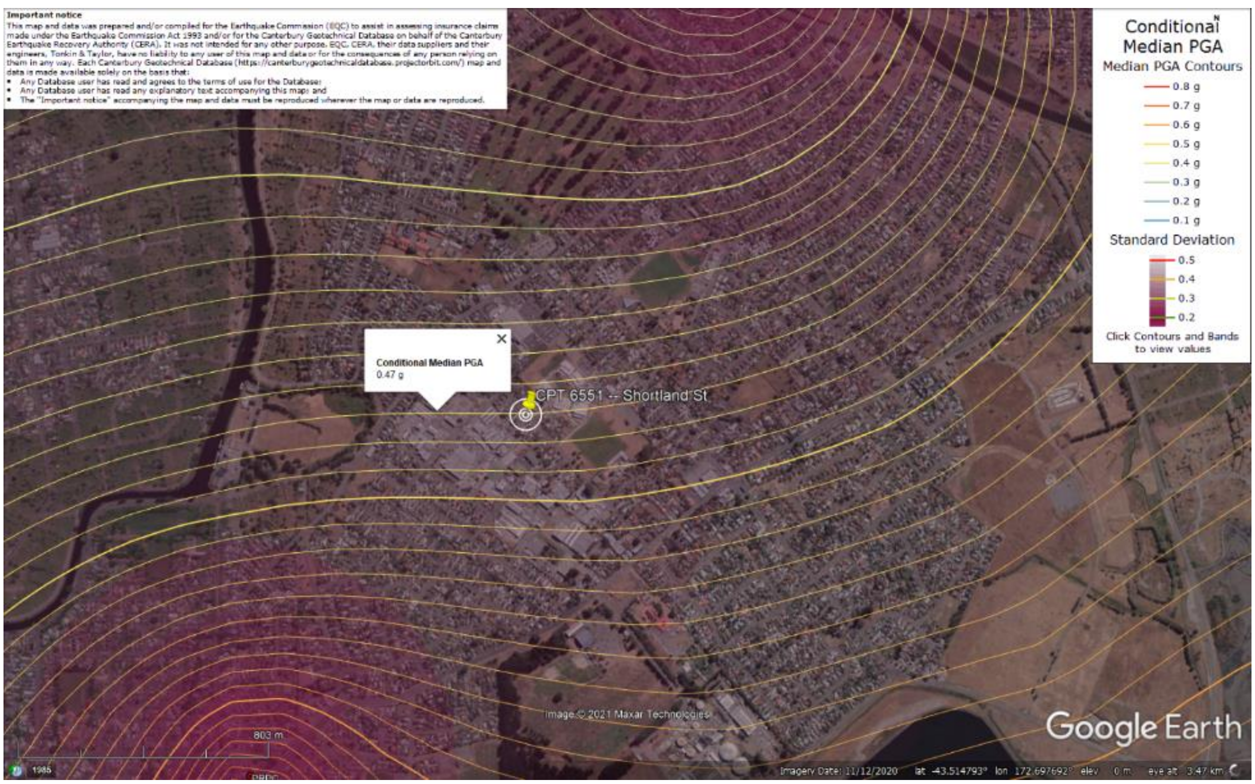

Figure 69: PGA for Feb-11 EQ (st. dev. = 0.325-0.350 ln units).

Figure 70: PGA for Jun-11 EQ (st. dev. = 0.325-0.350 ln units).

Figure 71: PGA for Dec-11 EQ (st. dev. = 0.375-0.400 ln units).

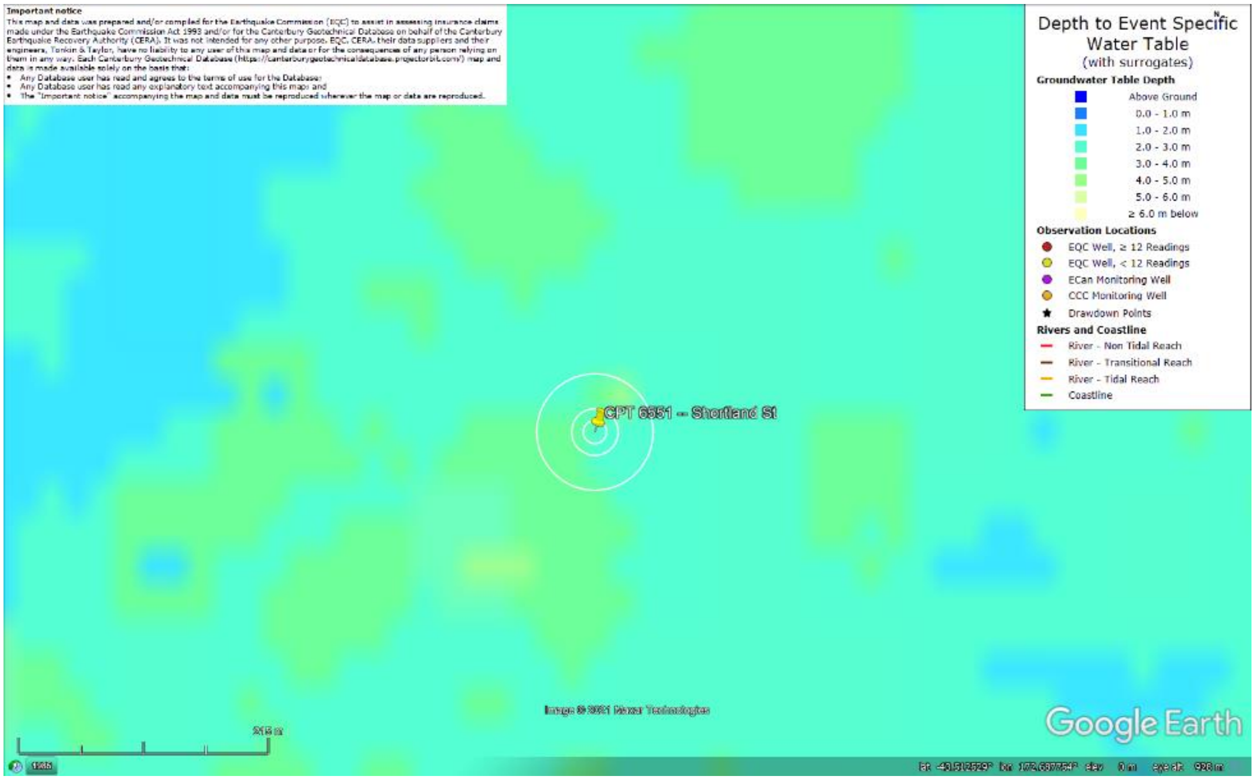

Figure 72: Depth to groundwater table for Sep-10 EQ.

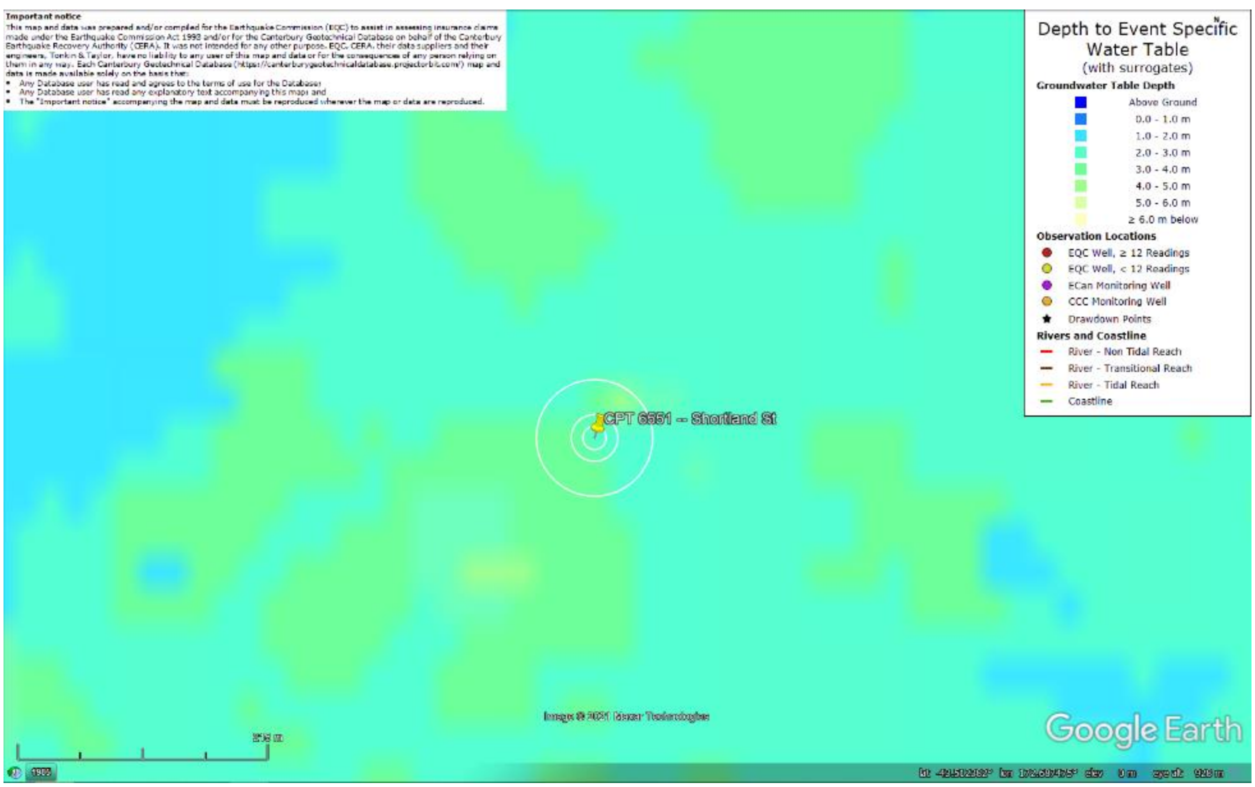

Figure 73: Depth to groundwater table for Feb-11 EQ.

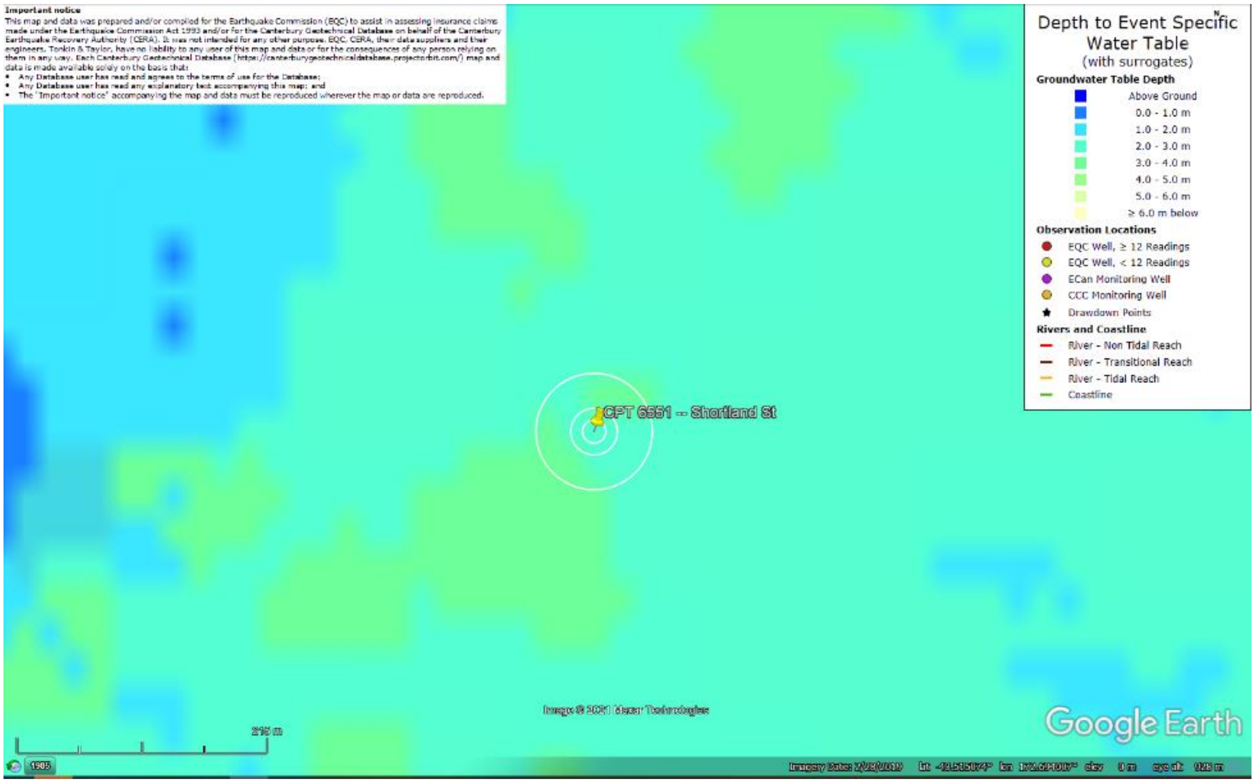

Figure 74: Depth to groundwater table for Jun-11 EQ.

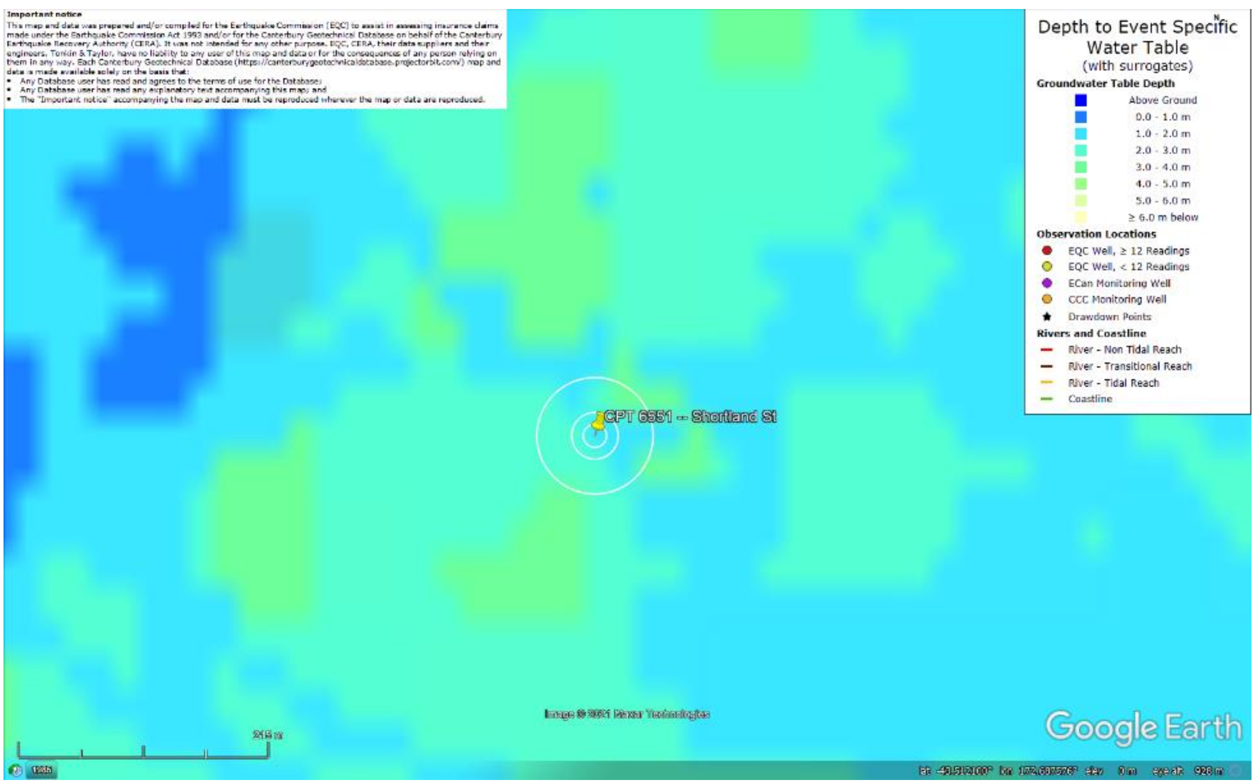

Figure 75: Depth to groundwater table for Dec-11 EQ.

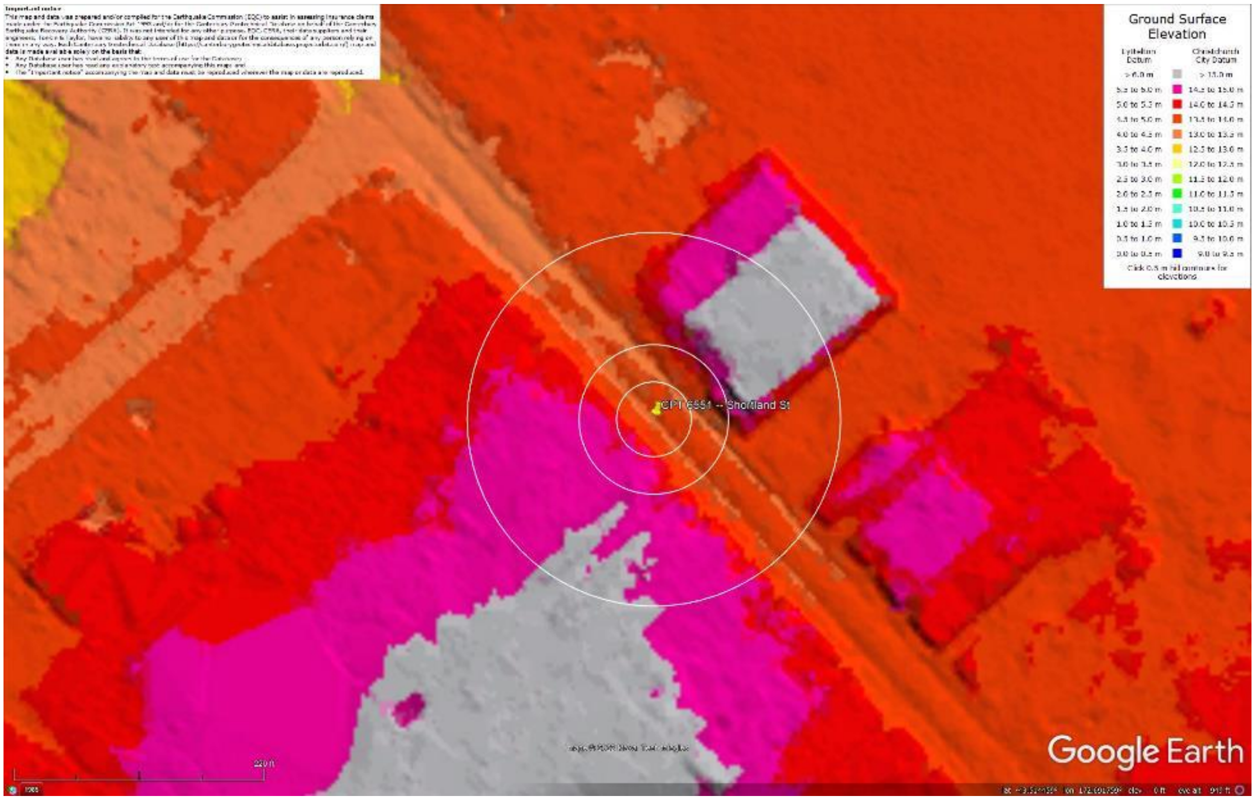

Figure 76: Ground surface elevation (Sep-11 LiDAR survey).

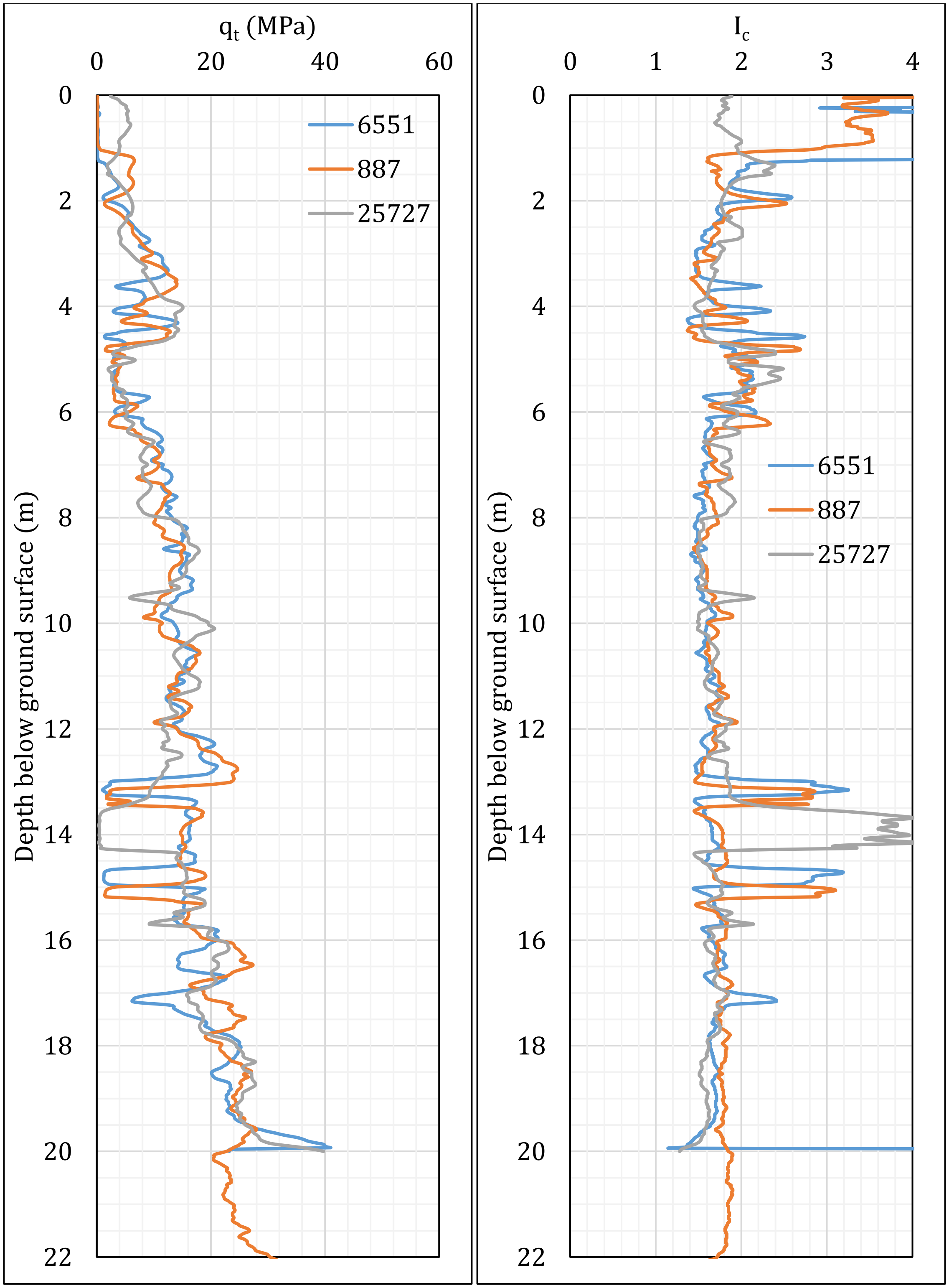

Figure 77: q_t and I_c profiles.

Note 6: The selection of CPTs for the area considered for settlement assessment (Figure 1) is based on the proximity of the CPTs to the considered areas. In accordance with that, the following table shows CPTs that were used for the volumetric settlement analysis in *Cliq v.3.0.3.2*, a CPT soil liquefaction software developed by GeoLogismiki. (The average volumetric settlements were reported in Table 8.)

Table 12: CPT profiles used in volumetric settlement analysis for areas selected for settlement assessment.

CPT ID No.	Patch A (10-, 20-, and 50-m buffers)	Road (20-m buffer)	Road (50-m buffer)
6551	✓	✓	✓
887	✓	✓	✓
25727			✓

Table 13: CPT-based results.

		CPT ID		
EQ Event	Parameter	6551	887	25727
Sep-10	S_{V1D} (mm)	10	15	18
	LSN	2	2	3
	LPI	0	0	0
	LPI_{ish}	0	0	0
	$D_{FS<1}$ (m)	undet.	undet.	undet.
Feb-11	S_{V1D} (mm)	110	103	143
	LSN	16	15	20
	LPI	10	11	14
	LPI_{ish}	4	4	4
	$D_{FS<1}$ (m)	3.58	3.92	3.02
Jun-11	S_{V1D} (mm)	40	50	59
	LSN	7	8	9
	LPI	2	3	2
	LPI_{ish}	0	0	0
	$D_{FS<1}$ (m)	4.70	4.90	5.06
Dec-11	S_{V1D} (mm)	65	75	93
	LSN	13	14	16
	LPI	4	5	6
	LPI_{ish}	0	0	0
	$D_{FS<1}$ (m)	4.61	2.01	2.74

Notes: $D_{FS<1}$ = Depth to the first liquefiable layer (FS_L<1) that is at least 200-mm thick, as determined by the Boulanger and Idriss (2016) liquefaction-triggering procedure (P_L=50%, C_{FC}=0.13, and $I_{c,cutoff}$ =2.6), and exported from *Cliq v.3.0.3.2*; undet. = the specified soil layer was not detected.

Note 7: Based on the borehole log (BH 15059, Figure 1), the groundwater table is at a depth of 1.5 m below the ground surface. The soil profile consists of (1) fine to medium sand, SP, of the Christchurch formation to a depth of 3.95 m, (2) silty fine to medium sand, SM, of the Christchurch formation to a depth of 4.4 m, (3) silt, ML, of the Christchurch formation to a depth of 5.45 m, and (4) fine to medium sand, SP, of the Christchurch formation to a depth of 20 m.

Note 8: The ejecta-induced free-field settlement provided in Table 11 is an areal average settlement due to ejecta, which is based on the total settlement assessment area, A_T (provided in Table 9 and repeated in Table 14). However, the considered area was not always covered completely with ejecta; thus, it is important to provide the localized ejecta-induced settlement, too. The localized settlement due to ejecta is estimated using photographic evidence only as

$$S_{E,P\_localized} = \frac{V_E}{A_E}$$

where V_E is the total volume of ejecta within A_T and A_E is the total coverage area of ejecta within A_T. Please note that the areal ejecta-induced settlement provided in Table 14 as S_{E,P_areal} is the same as $S_{E,P}$ in Table 11, which was estimated as

$$S_{E,P\_areal} = S_{E,P} = \frac{V_E}{A_T}$$

where V_E is the total volume of ejecta within A_T and A_T is the total settlement assessment area.

Table 14a: Areal and localized ejecta-induced settlement estimates for Road (20-m buffer) based on photographic evidence.

Earthquake Event	A_T (m^2)	A_E (m^2)	V_E (m^3)	S_{E,P_areal} (mm)	$S_{E,P\_localized}$ (mm)
Sep-10	430	0	0	0	0
Feb-11	430	430	9.0-13.7	25±5	25±5
Jun-11	418	418	7.2-12.1	25±5	25±5
Dec-11	430	0	0	0	0

Notes: S_{E,P_areal} = $S_{E,P}$ reported in Table 11 = areal ejecta-induced settlement; $S_{E,P\_localized}$ = localized ejecta-induced settlement; A_T = total settlement assessment area; V_E = total volume of ejecta within A_T; A_E = total area of ejecta within A_T; The estimates of both areal and localized ejecta-induced settlement are rounded to the nearest 5; Final plus/minus values are also rounded to the nearest 5.

Table 14b: Areal and localized ejecta-induced settlement estimates for Road (50-m buffer) based on photographic evidence.

Earthquake Event	A_T (m^2)	A_E (m^2)	V_E (m^3)	S_{E,P_areal} (mm)	$S_{E,P\_localized}$ (mm)
Sep-10	1102	0	0	0	0
Feb-11	1102	1102	28.9-45.6	35±5	35±5
Jun-11	1067	1067	24.7-39.8	30±5	30±5
Dec-11	1102	0	0	0	0

Notes: S_{E,P_areal} = $S_{E,P}$ reported in Table 11 = areal ejecta-induced settlement; $S_{E,P\_localized}$ = localized ejecta-induced settlement; A_T = total settlement assessment area; V_E = total volume of ejecta within A_T; A_E = total area of ejecta within A_T; The estimates of both areal and localized ejecta-induced settlement are rounded to the nearest 5; Final plus/minus values are also rounded to the nearest 5.

<u>Summary 2:</u>

The best estimate of the <u>localized</u> ejecta-induced settlement of the road at the Shortland St site for the SEP 2010, FEB 2011, JUN 2011, and DEC 2011 earthquake is 0 mm, 25±5 mm, 25±5 mm, and 0 mm, respectively.